AGU PUBLICATIONS

Tectonics

RESEARCH ARTICLE
10.1002/2014TC003809

Key Points:
- Zuccale Fault architecture is consistent with brittle deformation
- Radiometric data bracket fault activity between 6.3 and 5.3 Ma
- Slip was enhanced by cyclic presence of high pore fluid pressures

Supporting Information:
- Readme
- Table S1

Correspondence to:
G. Musumeci,
gm@dst.unipi.it

Citation:
Musumeci, G., F. Mazzarini, and A. R. Cruden (2015), The Zuccale Fault, Elba Island, Italy: A new perspective from fault architecture, *Tectonics*, *34*, 1195–1218, doi:10.1002/2014TC003809.

Received 19 DEC 2014
Accepted 25 MAY 2015
Accepted article online 29 MAY 2015
Published online 21 JUN 2015

The Zuccale Fault, Elba Island, Italy: A new perspective from fault architecture

G. Musumeci[1,2], F. Mazzarini[2], and A. R. Cruden[3]

[1]Dipartimento di Scienze della Terra, Università di Pisa, Pisa, Italy, [2]Istituto Nazionale di Geofisica e Vulcanologia, Pisa, Italy, [3]School of Earth, Atmosphere and Environment, Monash University, Melbourne, Victoria, Australia

Abstract The Zuccale Fault, central-eastern Elba Island, has been regarded since the 1990s as a low-angle normal fault that records Neogene crustal extension in the inner (Tyrrhenian side) portion of the northern Apennines. The flat-lying attitude of the fault zone and the strong excision of thick nappes were the main reasons for this interpretation. Previous structural and petrographic studies have focused primarily on the fault rocks themselves without map-scale investigation of the structural setting and deformation structures in the hanging wall and footwall blocks. Furthermore, despite the complex history proposed for the Zuccale Fault, the timing of deformation has not yet been constrained by radiometric age data. We present the findings of recent geological studies on eastern Elba Island that provide significant new insight on the nature and tectonic significance of the Zuccale Fault. We document in detail the architecture of breccias and cataclasites that comprise the Zuccale Fault. Our new observations are consistent with a purely brittle deformation zone that crosscuts older early-middle and late Miocene regional and local tectonic structures. The activity on the fault postdates emplacement of the late Miocene Porto Azzurro pluton, and it displaces a previously formed nappe stack ~6 km eastward without any footwall exhumation or hanging wall block rotation. These new data raise questions about the development of misoriented faults in the upper crust.

1. Introduction

Current thinking on the Neogene tectonic evolution of northern Apennines (Figure 1a) suggests that, since the early Miocene, the internal zone of the Apennine chain, namely, the Tyrrhenian Domain, has been characterized by the eastward migration of two coupled, NW-SE striking, active deformation belts [e.g., *Carmignani et al*., 1994]. Since the early Miocene, a frontal contractional belt has coexisted with a subparallel extensional belt within the hinterland sector [e.g., *Elter*, 1975; *Barchi et al*., 2006]. As a consequence of this migration pattern, all sectors of the Tuscany-Umbria region have undergone a compressional tectonic phase followed by later extension. According to *Keller and Coward* [1996] and *Collettini and Holdsworth* [2004], this crustal extension has been in part accommodated by low-angle normal faults (LANFs). The Zuccale Fault [*Keller and Coward*, 1996; *Collettini and Holdsworth*, 2004], in the inner portion of the belt (Figure 1a), is the oldest known potential LANF, whereas the currently active Altotiberina fault in the external portion of the belt (Figure 1a) is the youngest [*Boncio et al*., 2000; *Mirabella et al*., 2011].

Two characteristics make the Zuccale Fault the only LANF in the northern Apennines where fault dynamics can be analyzed: (1) both the hanging wall and footwall rocks are exposed either side of a subhorizontal (flat) fault segment and (2) the net slip in these segments is geologically well defined.

Progress in understanding the nature and significance of the Zuccale Fault has been limited because (1) previous structural and petrographic studies have focused on the fault rocks alone, without any investigation of the regional structural setting or deformation and metamorphic evolution of the hanging wall and footwall rocks and (2) despite the complex history proposed for this structure, the timing of both fault and footwall deformation is not constrained by radiometric age data.

To bridge these current gaps in knowledge, we present the findings of new detailed geological studies on central-eastern Elba Island that provide significant new insight into the architecture and internal deformation of the Zuccale Fault and its evolution through time. After summarizing the published literature, we present results of recent geological and structural mapping in eastern Elba Island and finally

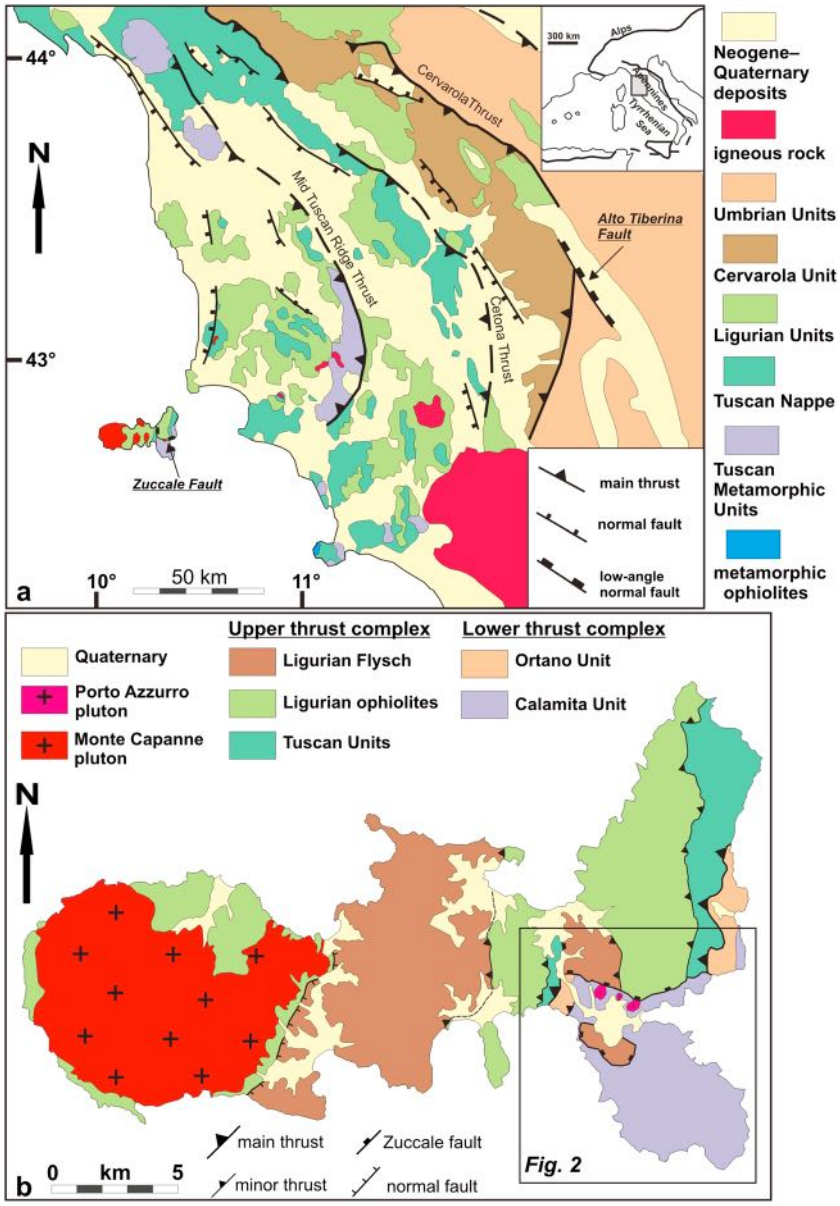

Figure 1. (a) Tectonic sketch map of the northern Apennines with locations of main tectonic structures (after *Boccaletti and Sani* [1998]) and (b) geological sketch map of Elba Island (modified after *Mazzarini et al.* [2011]).

discuss the implications of the new data for a revised architecture and alternative interpretation for the Zuccale Fault. In particular, the revised architecture of Zuccale Fault addresses the problem of frictional behavior and slip along low-angle faults at upper crustal level [e.g., *Axen*, 2004; *Collettini*, 2011].

2. Geological Outline

The northern Apennines (Figure 1a) are a Cenozoic orogenic belt formed by progressive eastward thrust stacking of oceanic (Ligurian) and Adria continent-derived (Tuscan) units, driven by the westward subduction of the Adria microplate beneath the European plate (Corso-Sardinian block [*Boccaletti et al.*, 1971; *Elter*, 1975]). Crustal deformation began in the Eocene, affecting first the inner oceanic domains (Ligurian and Subligurian Domains) and then continuing in the late Oligocene-early-middle Miocene to involve the proximal side of the Adria continental margin (Tuscan Domain) and progressively more external zones in the late Miocene-Pliocene.

The inner (Tyrrhenian) margin of the northern Apennines consists of the following tectonic units from top to bottom:

Ligurian Units: remnants of the Mesozoic Liguro-Piemontese Ocean [*Elter*, 1975], made up of Jurassic ophiolites covered by Upper Jurassic-Paleocene deepwater sediments and Cretaceous-Paleocene flysch sequences. These units were deformed at very shallow structural levels under subgreenschist facies conditions.

Tuscan Units: Adria-derived continental rocks deformed at different structural levels: (i) the Tuscan Nappe, made up of nonmetamorphic to very low grade metamorphic rocks of Late Triassic to early Miocene age, and (ii) the Tuscan metamorphic units, comprising Paleozoic basement rocks and Permian-Triassic or Late Triassic-Oligocene metamorphic sequences.

The metamorphic units crop out along an arcuate belt from the Apuan Alps in the north to Monte Argentario at the south (Figure 1a), and they experienced polyphase deformation under high-pressure/low-temperature (HP/LT) metamorphic conditions ranging from greenschist facies (0.6–0.8 GPa [*Molli et al*., 2002]) to blueschist facies (1–1.2 GPa [*Giorgetti et al*., 1998; *Theye et al*., 1997]). Their deformation history is recorded by early structures associated with underthrusting and synmetamorphic folding and nappe stacking, followed by overprinting structures related to exhumation and uplift [*Carmignani and Kligfield*, 1990].

Since the late Miocene, the inner margin of the northern Apennines has been the site of localized crustal melting and magmatism (Tuscan Magmatic Province [*Serri et al*., 1993]). The most common products are felsic intrusive rocks, a large volume of which consists of Pliocene-Pleistocene intrusions, emplaced at depths of 3–5 km in the currently active Larderello geothermal field [*Bertini et al*., 2006]. In the northern Tyrrhenian Sea, 8.4–4.8 Ma intrusive and volcanic rocks crop out on the islands of Elba, Capraia, Montecristo, and Giglio [*Dini et al*., 2002; *Rosenbaum et al*., 2008, and references therein]. Tuscan magmatism is currently explained in the context of crustal extension related to late Miocene-Pliocene opening of the Tyrrhenian Sea as a back-arc basin [*Malinverno and Ryan*, 1986; *Carmignani et al*., 1994; *Keller and Coward*, 1996; *Jolivet et al*., 1998; *Rosenbaum and Lister*, 2004]. However, the model of crustal extension in the northern Apennines remains contentious. For example, several structural studies document Pliocene regional-scale crustal shortening with associated coeval magmatism [*Boccaletti et al*., 1997; *Boccaletti and Sani*, 1998; *Cerrina Feroni et al*., 2006; *Musumeci et al*., 2008].

2.1. Elba Island

Elba Island is made up of five tectonic units that were stacked northeastward during the early-middle Miocene (Figure 1b) and subsequently intruded by late Miocene plutons and sills [*Barberi et al*., 1967; *Pertusati et al*., 1993; *Keller and Coward*, 1996]. The five tectonic units are subdivided into lower and upper thrust complexes [*Musumeci and Vaselli*, 2012], separated by a main thrust zone that is marked by a strongly tectonized decameter-thick slices of serpentinites [*Keller and Coward*, 1996]. The main thrust zone is represented by the Capo Norsi thrust in central Elba and by the Monte Arco thrust in eastern Elba Island (Figures 2a and 2b).

The upper thrust complex (Figure 1b) consists of three thrust sheets comprising sedimentary and/or very low grade metamorphic rocks belonging to the Ligurian Units and the Tuscan Nappe. From bottom to top, they correspond to (i) Tuscan Units: low metamorphic grade Permian-Triassic siliciclastic rocks followed upward by Late Triassic-Jurassic carbonate rocks, (ii) Ligurian ophiolites: Mesozoic ophiolitic and sedimentary cover rocks with an internal Ligurian affinity, and (iii) Ligurian flysch: Upper Cretaceous flysch and Paleocene/Eocene flysch with an external Ligurian affinity.

The lower thrust complex (Figures 1b and 2a) comprises the metamorphic Calamita and Ortano Units. The Calamita Unit is made up of high- and medium-grade pelitic-psammitic hornfels derived from Early Carboniferous flysch (Calamita Schists) [*Musumeci et al*., 2011], which is overlain by Middle Triassic metasandstones (Verrucano Formation) and Early Jurassic carbonate rocks (Calanchiole Marble [*Garfagnoli et al*., 2005]). The Ortano Unit comprises, from bottom to top, (i) Middle Ordovician low-grade metasandstone and metavolcanic rocks (Ortano Porphyroid [*Musumeci et al*., 2011]), (ii) a thin slice of Early Jurassic(?) dolomitic marble (Ortano Marble), and (iii) Early Cretaceous medium- and high-grade pelitic and carbonate hornfelses (Acquadolce Unit [*Pertusati et al*., 1993]).

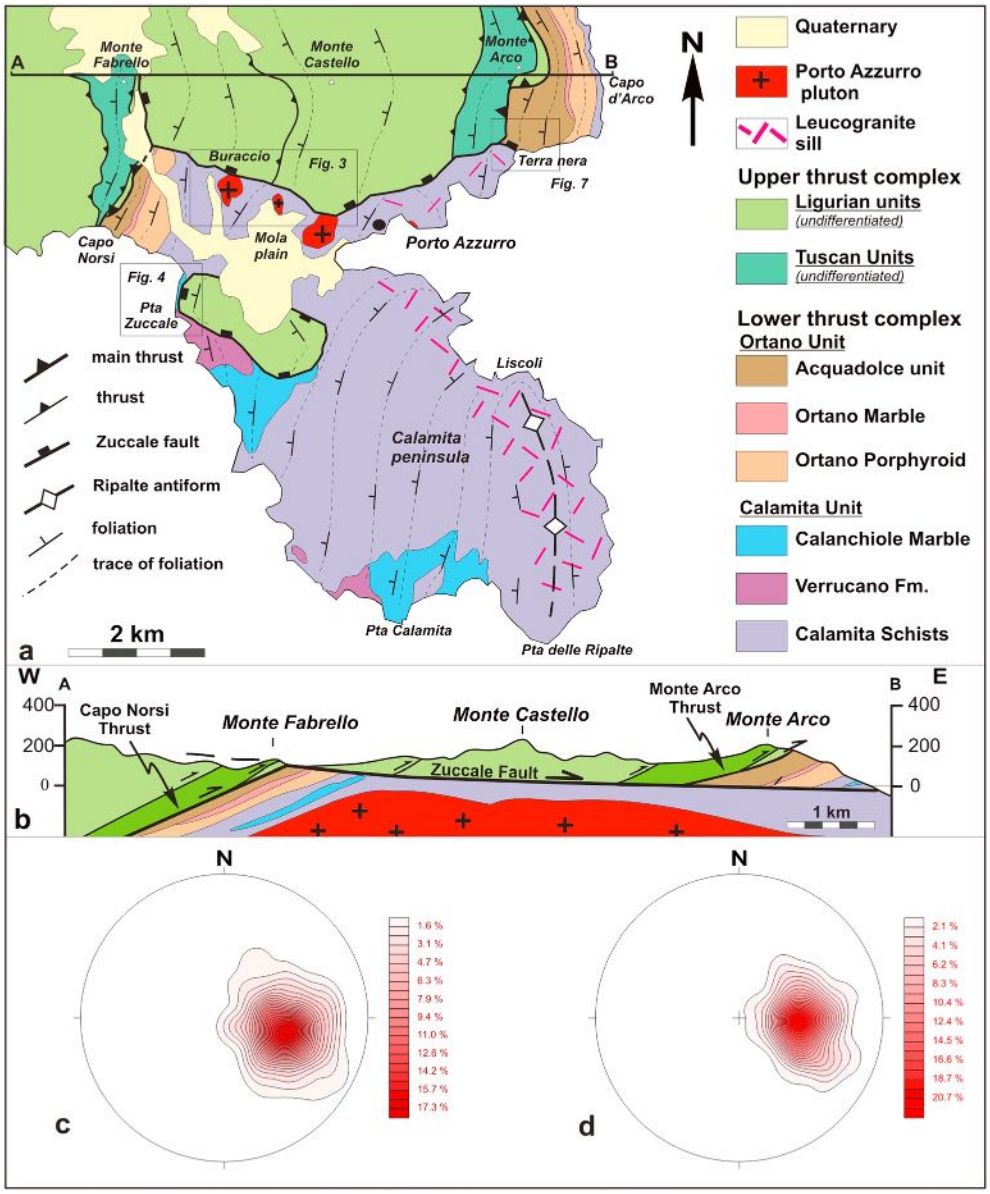

Figure 2. (a) Geological sketch map of thrust complexes in southeastern Elba, (b) cross section from central to eastern Elba Island, (c) contoured equal-area lower hemisphere projections of poles to metamorphic foliation in the footwall block of Zuccale Fault, and (d) contoured equal-area lower hemisphere projections of poles to sedimentary bedding and axial plane cleavage in the hanging wall block of Zuccale Fault.

According to *Pertusati et al.* [1993] and to *Keller and Coward* [1996], the tectonic evolution of Elba Island can be summarized in two stages. The early stage of folding and thrust stacking, constrained to approximately 19 Ma in the Ortano Unit [*Deino et al.*, 1992], developed under very low metamorphic grade conditions in the upper complex and low metamorphic grade conditions in the lower complex. Thrust structures recognizable in central-eastern Elba Island strike NS and dip moderately west defining a large-scale monocline [*Keller and Coward*, 1996]. Thrust-related mesoscopic folds have axes oriented from N-S to NNE-SSW in the lower complex, whereas in the upper complex fold axis directions range from NNW-SSE to NNE-SSW with an arcuate geometry that is subparallel to the basal thrust (Mount Arco thrust in eastern Elba; Figures 1b and 2).

The second stage of the tectonic evolution of Elba Island is characterized by late Miocene magmatism, with multiple intrusive events from about 8 to 5.9 Ma that led to the emplacement of two large composite plutonic

bodies, leucogranitic sills and laccoliths into the nappe stack [*Dini et al*., 2002]. The Monte Capanne pluton in the west and the Porto Azzurro pluton in the east were emplaced into the upper and lower thrust complexes, respectively, and are associated with medium- to high-grade contact metamorphic aureoles [*Bouillin*, 1983; *Duranti et al*., 1992; *Rossetti et al*., 2007; *Musumeci and Vaselli*, 2012]. Magma emplacement was accompanied by coeval host-rock deformation with the development of folds and fault zones, which have been previously attributed to (i) the collapse of the tectonic stack during pluton ballooning [*Pertusati et al*., 1993; *Garfagnoli et al*., 2005] or (ii) crustal extension [*Keller and Coward*, 1996]. In this context, the Zuccale Fault (Figures 1b and 2) has been interpreted to be an east dipping low-angle fault ($<10°$), roughly coeval with granite emplacement, which crosscuts the nappe pile displacing hanging wall units ~6 km to the east [*Pertusati et al*., 1993; *Keller and Coward*, 1996; *Smith et al*., 2011a].

Detailed investigations of the relationships between structures and pluton emplacement in southeastern Elba have recently reported the occurrence of large-scale N-S trending upright folds (Ripalte antiform in Figure 2a) that deformed the contact aureole of the Porto Azzuro pluton and controlled the circulation of high-temperature hydrothermal fluids (tourmaline veins [*Mazzarini et al*., 2011]). Moreover, on the western side of the Porto Azzurro pluton, west dipping ductile reverse shear zones (Calanchiole shear zone and Felciaio shear zone) within carbonate units in the lower thrust complex (Calanchiole and Ortano marbles) also led to tectonic repetition of the contact aureole [*Musumeci and Vaselli*, 2012]. These shear zones are marked by syncontact metamorphic protomylonitic to mylonitic fabrics developed during retrogression of the contact metamorphic aureole from pyroxene hornfels facies to hornblende and albite-epidote hornfels facies, with fine-grained tremolite-talc-calcite mylonitic marble representing the latest fabric [*Musumeci and Vaselli*, 2012].

Deformation features (folds and shear zones) are widely distributed within the contact aureole of the Porto Azzuro pluton throughout the Calamita Peninsula and adjoining areas. In particular, the large amplitude of the Ripalte antiform (Figure2a) and its steeply dipping axial plane are consistent with subhorizontal compression, which has been used to suggest that pluton emplacement occurred during crustal shortening [*Mazzarini et al*., 2011; *Musumeci and Vaselli*, 2012]. Recent field and microstructural research indicates that the Capo d'Arco Schist (Figure 2), previously assigned to the Ortano Unit [*Duranti et al*., 1992], should be included in the Calamita Unit due to the presence of diagnostic cordierite-andalusite-bearing mineral assemblages and leucogranitic sills [*Mazzarini et al*., 2011; *Musumeci and Vaselli*, 2012].

3. The Zuccale Fault: Previous work

The Zuccale Fault (Figure 2) was first described as a low-angle detachment fault by *Keller and Pialli* [1990]. According to *Keller and Coward* [1996], the main structural characteristics of the Zuccale Fault are:

1. It is an east dipping low-angle fault ($<10°$) that cuts downsection, displacing Apennine nappes by up to 6 km.
2. The fault zone has a planar geometry, strong lateral thickness variations (average thickness 5 m), and contains a variety of fault rock types including breccias, gouges, and cataclasites.
3. Planar fabrics in the fault comprise (1) west to northwest dipping foliation defined by preferred orientation of phyllosilicates in clay-rich gouge, (2) subhorizontal shear planes at the contact between gouge and intact rock, and (3) east to southeast dipping Riedel shears.
4. Strong linear fabrics (subhorizontal skickenside lineations and crystal fiber lineations) and associated asymmetric structures are consistent with a dominant top-to-the-east to southeast slip direction.

There have been a significant number of structural studies on the dynamic and kinematic significance of the Zuccale Fault over the last decade [e.g., *Collettini and Holdsworth*, 2004; *Collettini et al*., 2009; *Collettini*, 2011; *Smith and Faulkner*, 2010; *Smith et al*., 2011a, 2011b]. *Collettini and Holdsworth* [2004] emphasized the role of the Zuccale Fault as the main structure accommodating late Neogene crustal extension in the upper crust of the northern Apennines and proposed a possible mechanical explanation for its development as a LANF. They also reported a zonation of fault rocks characterized by cataclastic textures overprinted by a foliated phyllosilicate-rich (mylonite) fabric in the core of the fault, indicating fault activity that started with pervasive cataclasis, which enhanced permeability and the influx of CO_2-rich hydrous fluids [*Collettini and Holdsworth*, 2004]. This triggered low-grade alteration and the onset of pressure solution as the dominant grain-scale deformation mechanism in the cataclasites, leading to shear localization and formation of talc-rich mylonitic layers in the fault core. This in turn promoted rock weakening and a switch from frictional to frictional-viscous fault behavior [e.g., *Collettini et al*., 2009]. *Smith et al.* [2011b] subsequently reported an alternative

deformation history with early development of mylonitic fabrics (talc phyllonite) followed by cataclastic fabrics (cataclasites and breccias).

4. New Structural Data From the Zuccale Fault

The Zuccale Fault is exposed for several kilometers between Monte Fabrello in the west and Terra Nera in the east (Figure 2a). In cross section the same sequence of tectonic units occurs in the footwall and hanging wall blocks (Figure 2b). In particular, the recent reassignment of the Capo d'Arco Schist to the Calamita Unit [*Mazzarini et al*., 2011] indicates that high metamorphic grade portions of the Porto Azzurro pluton's contact aureole occur in both footwall and hanging wall blocks. Foliations and tectonic structures have the same attitude in the footwall and hanging wall blocks (Figures 2c and 2d). An eastward horizontal displacement of ~6 km is estimated by using the thrust between the upper and lower thrust complexes (Capo Norsi thrust in the footwall and Monte Arco thrust in the hanging wall) as pre-Zuccale displacement markers (Figure 2b). The greatest tectonic excision (attenuation of nappe-stack thickness) occurs in the western segment of the fault zone (Monte Fabrello-Buraccio area) where the uppermost tectonic unit (Ligurian Cretaceous flysch) in the hanging wall lies above the lowermost tectonic unit (Calamita Schist of the Calamita Unit) in the footwall (Figures 2a and 2b). Tectonic excision of the nappe stack decreases progressively to the east until it dies out in the easternmost segment of the fault (east of Mount Arco; Figures 2a and 2b), where the Calamita Unit occurs in the hanging wall and footwall. It is also noteworthy that we have not observed coeval steeply dipping normal faults and/or backrotated faults in the hanging wall block that root into the Zuccale Fault zone. Furthermore, all observed fracture zones and high-angle faults with decimeter to meter displacements in the hanging wall either abut or crosscut the Zuccale Fault. The following detailed descriptions of the Zuccale Fault and its footwall and hanging wall focus on new structural data from three key areas in eastern Elba Island, namely, the (i) Buraccio-Mola, (ii) Calanchiole-Punta di Zuccale, and (iii) Terra Nera sections (Figures 3, 4, and 7, respectively).

4.1. Buraccio-Mola Section

In this section, the relationship between tectonic units in the hanging wall and footwall of the Zuccale Fault and the fault itself can be observed over an east-west strike distance of ~3 km (Figure 3a).

The footwall units comprise the Calamita Schist, Calanchiole Marble, and felsic igneous rocks of the Porto Azzurro monzogranite. Both the Calamita Schist and Calanchiole Marble consist of medium-grade hornfels (hornblende-hornfels facies) with andalusite-bearing mineral assemblages in pelitic-psammitic rocks (Calamita Schist) and coarse-grained recrystallized fabrics in the Calanchiole Marble. The dominant fabric is a moderately W to WNW dipping foliation (Figures 3a and 3e) defined by intense recrystallization and growth of medium-grade mineral assemblages. A mineral lineation is defined by aligned andalusite porphyroblasts (0.5–0.8 cm in size) and biotite aggregates. The foliation and hornfels schist are folded by gently N to NE plunging metric- to decametric-scale folds (Figure 3e). At map scale the most important folds are represented by two asymmetric, overturned synclines with moderately NNW dipping axial planes cored by the Calanchiole Marble (Figures 3b–3d). Similar large-scale inclined to overturned folds have been recognized in the Calamita Peninsula, affecting the main foliation and contact metamorphic assemblages in the Calamita Schist [*Mazzarini et al*., 2011; *Musumeci and Vaselli*, 2012].

In the hanging wall the Ligurian Units unaffected by metamorphism define a west dipping homocline of tectonic slices with N-S striking west dipping tectonic contacts (Figures 3a–3d); from bottom to the top they consist of Jurassic ophiolite (diabase) and related sedimentary cover rocks (Calpionelle limestone), followed by Paleocene flysch and Upper Cretaceous Helminthoid flysch. Both flysch units are intruded by late Miocene 7–8 Ma aplitic and porphyritic leucogranite sills [*Dini et al*., 2002].

The main planar fabric in the Calpionelle limestone and Helminthoid flysch corresponds to bedding and/or a crenulation cleavage, which is axial planar to N to NW plunging decimetric to metric upright, open folds (Figure 3f).

The Zuccale Fault in the Buraccio-Mola section is subhorizontal (map-scale average dip $< 5°$), discordant to footwall and hanging wall structures and separates the lowermost and uppermost tectonic units of the Elba Island nappe stack (Figures 3c and 3d). In the footwall the fault truncates the contact between the Porto Azzurro pluton monzogranite (5.9 Ma [*Maineri et al*., 2003]) and its folded host rocks. In the hanging

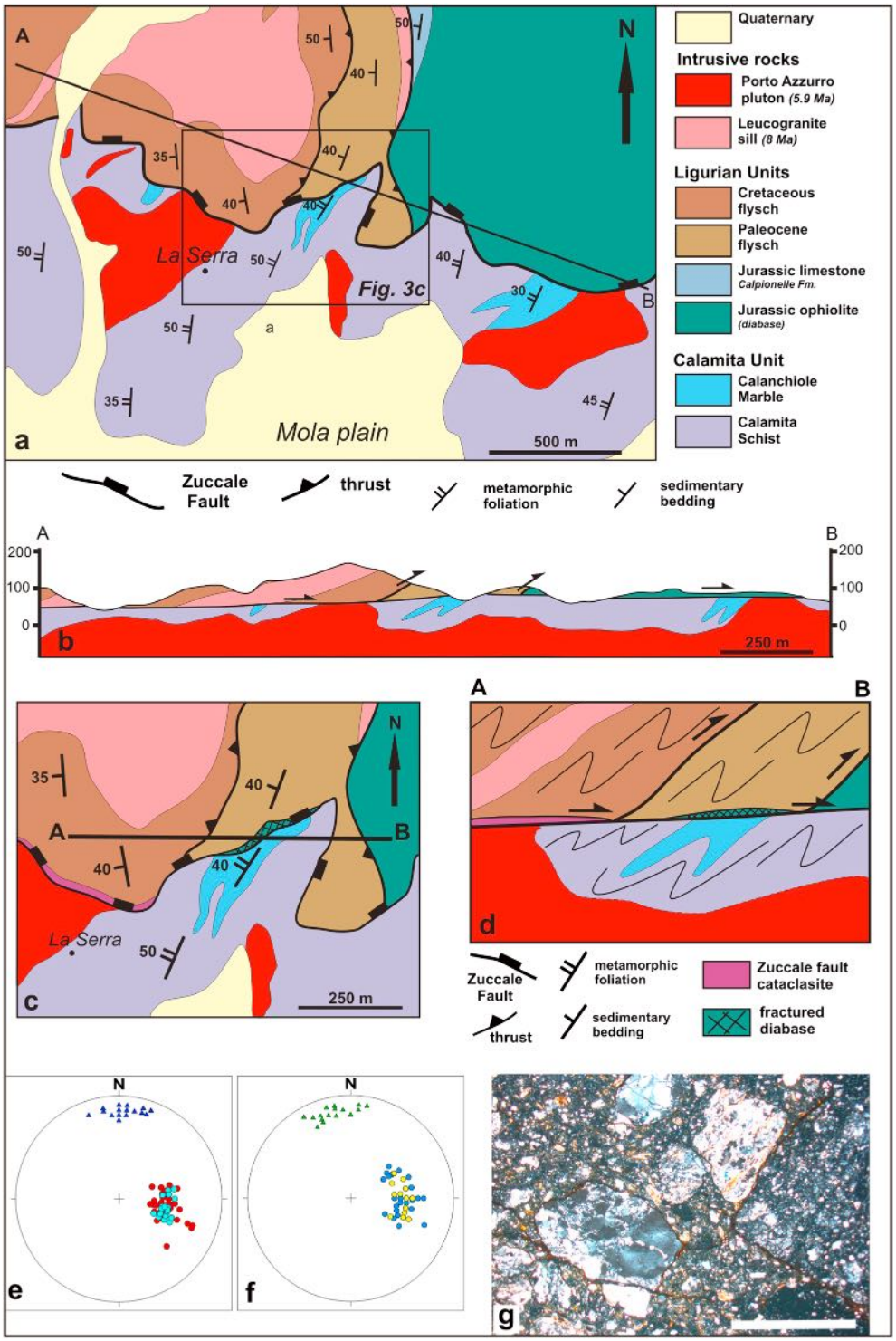

Figure 3. Buraccio-Mola section (see location in Figure 2a). (a) Geological sketch map and (b) cross section of examined section of Zuccale Fault; (c and d) detailed map and schematic cross section showing attitude of Zuccale Fault and relationships with rock units and structures; (e) Calamita Unit: equal-area lower hemisphere projections of poles to metamorphic foliation (red dots), poles to axial planes (light blue dots), and fold axes (blue triangles); (f) Ligurian Unit: equal-area lower hemisphere projections of poles to sedimentary bedding (blue dots), poles to axial planes (yellow dots), and fold axes (green triangles); and (g) photomicrograph of fault breccia at the base of Zuccale Fault, with clasts of intrusive and metamorphic rocks derived from the footwall Calamita Unit; scale bar: 2 mm.

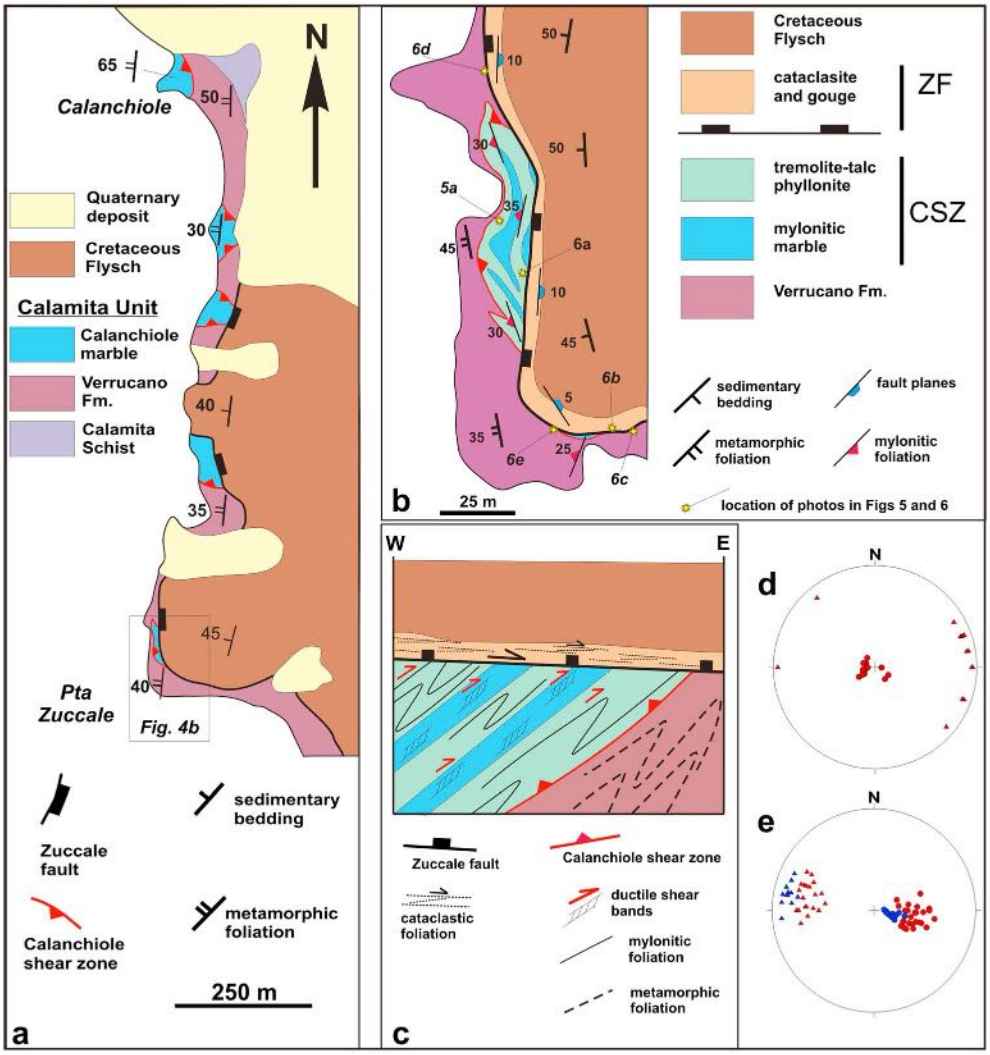

Figure 4. Punta di Zuccale section (see location in Figure 2a). (a) Geological sketch map of Calanchiole-Punta di Zuccale area showing map-scale relationships between the Calanchiole shear zone and the Zuccale Fault; (b and c) detailed map and schematic cross section showing architecture and fault rock distribution in the Calanchiole shear zone and Zuccale Fault; (d) Zuccale Fault, equal-area lower hemisphere projections of poles to fault planes (red circles) and slickenside lineations (red triangles) in the breccias and cataclasites; and (e) Calanchiole shear zone, equal-area lower hemisphere projections of poles to mylonitic foliation (red circles), shear bands (blue circles), mylonitic lineations (red triangles), and slickenside lineations (blue triangles).

wall, the fault zone truncates west dipping thrusts. The sharp transition (1–3 m) from footwall to hanging wall rocks throughout the section indicates that the fault zone is 1 to 2 m thick (Figure 3c). Fault rocks consist mainly of greyish matrix-supported breccias (in the sense of *Wise et al.* [1974]) with rounded to subrounded clasts (average size 2–0.5 mm) of hornfels, coarse-grained quartzite, and felsic intrusive rocks embedded in a very fine grained (30–50 μm) phyllosilicate-rich matrix (Figure 3g). The clast compositions indicate derivation from the Calamita Schist and Porto Azzurro pluton of the footwall. Farther east, the Zuccale Fault is marked by a meter-thick slice of highly fractured diabase that is tectonically sandwiched between the Calanchiole Marble in the footwall and black shale and limestone of the Paleocene flysch in the hanging wall (Figures 3c and 3d). Close to the fault zone, limestone layers within Upper Cretaceous flysch are affected by intense brecciation as previously reported by *Keller and Coward* [1996].

4.2. Punta di Zuccale Section

Along the western side of Calamita Peninsula (Figures 2a and 4a), lithological units and tectonic structures of the footwall block (here Verrucano hornfels schist and mylonitic marble of the Calanchiole shear zone) are

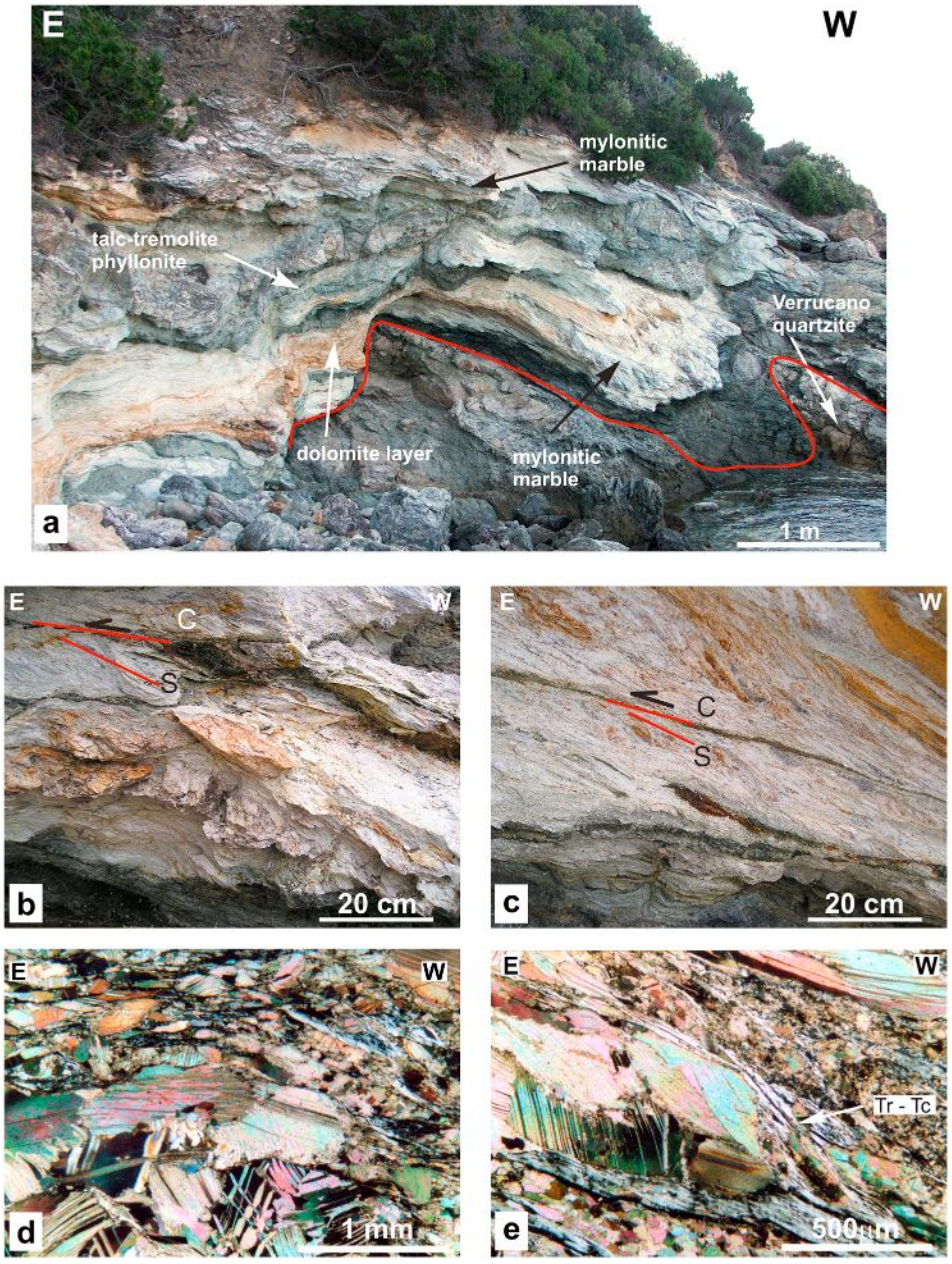

Figure 5. Punta di Zuccale section, Calanchiole shear zone. (a) Mylonitic marbles and talc-tremolite phyllonite in contact with underlying quartzites of Verrucano Formation. The contact is marked by breccias and dark green layer made up of fractured/brecciated calcsilicate. Details of mylonitic marbles with (b) west dipping SC foliation wrapping around decimeter-thick pods of coarse-grained poorly deformed dolomitic marble and (c) thin tremolite-rich shear bands (green layers) in the most deformed portion of mylonitic marbles. (d) Photomicrograph showing detail of coarse-grained fabric in a marble pod crosscut by thin tremolite-rich fine grained foliation. (e) Detail of mylonitic foliation with alternation of very fine grained (<50 μm) calcite and tremolite-talc-rich layers wrapping around strained porphyroclasts of coarse-grained (>0.5 mm) calcite.

continuously exposed over ~1 km along the coast from Calanchiole to Punta di Zuccale (Figure 4a). At Punta di Zuccale, mesoscale relationships between the Zuccale Fault and footwall and hanging wall structures can be examined in detail along two N-S and E-W striking continuous sections totaling ~200 m of exposure (Figures 4b, 5a, and 6a).

4.2.1. Footwall and Hanging Wall Rocks

The footwall rocks at Punta di Zuccale are characterized by the occurrence of the 2–4 m thick Calanchiole shear zone [*Musumeci and Vaselli*, 2012], which consists of tremolite-talc phyllonite and mylonitic marble

with strong lateral variations in composition and thickness (Figures 4b and 5a). West dipping mylonitic foliations and shear bands with top to the east sense of shear form the dominant fabrics (Figures 4c, 4e, 5b, and 5c). The tremolite-talc phyllonite (Figure 5a) consists of grayish green phyllonites with whitish carbonate layers and dark green massive layers. It strikes NS and has a foliation dipping moderately to the west (30°–50°), defined by the preferred orientation of very fine grained tremolite and/or tremolite + talc mineral assemblages that envelop porphyroclasts of coarse-grained amphibole (tremolite) and pyroxene (diopside) aggregates. Thin layers of mylonitic to ultramylonitic marble within the tremolite-talc phyllonite have oblique foliations and S-C texture, both of which indicate top-to-the-east sense of shear (Figure 4e). Mylonitic marbles occur as decimeter- to meter-thick lenses of mylonitic to ultramylonitic calcite-dolomite marble embedded within tremolite-talc-phyllonite (Figure 5a). At the mesoscopic scale the mylonitic fabric is defined by very fine grained calcite layers associated with discontinuous 1 to 3 mm thick tremolite-rich lamellae, wrapping around centimetric coarse- to medium-grained calcite and/or calcite-dolomite-rich layers (Figures 5b and 5c). In thin section, the mylonitic fabric consists of very fine grained, equigranular, strain-free calcite grains (30–60 μm) and very fine grained tremolite layers. Coarse-grained porphyroclasts (Figures 5d and 5e) consist of highly strained calcite grains with shape-preferred orientation or coarse-grained calcite grains with undulose extinction, deformation bands, and high twin lamellae density (Figure 5d). Millimeter- to centimeter-thick, homogeneous, light-colored ultramylonitic layers characterized by very fine grained (20–30 μm), equigranular, and strain-free calcite grains and lack of porphyroclasts are the highest strain component in the core of the Calanchiole shear zone. Within tremolite-talc phyllonite and/or mylonitic marble, discontinuous centimeter-thick dark green layers with lenticular shapes and massive fabric correspond to coarse-grained hydrothermal skarn with epidote + amphibole (mostly tremolite) + albitic plagioclase assemblages.

The hanging wall rocks of the Zuccale Fault consist of moderately west dipping, nonmetamorphic black claystones and limestones of the Cretaceous flysch (external Ligurian Unit) (Figure 4b). Similarly to the Buraccio section described above, the limestone layers close to the contact with the fault zone are affected by brecciation and calcite veins.

4.2.2. The Fault Zone

The Zuccale Fault consists of a 1.5 to 3 m thick brittle fault zone that discordantly crosscuts all footwall (Verrucano hornfels schist and mylonitic marble) and hanging wall (Upper Cretaceous flysch) rocks units (Figures 4a–4c, 6a, and 6b). Of particular relevance within the NS cross section is the exposure of a tectonic discordance between the gently east dipping (5°–10°) Zuccale Fault zone and the underlying west dipping (40°–45°) mylonitic marble of the Calanchiole shear zone (Figures 4b, 4c, and 6a). Additionally, a meter-thick slice of mylonitic marble as well as a calc-silicate layer are tectonically pinched out in the fault zone, as exposed in a small cave within the EW cross section.

Fault rocks are matrix-supported breccias and greyish/yellowish cataclasites with centimeter-thick gouge layers (Figures 6b, 6c, 6e, and 6f). East dipping clay-rich shear planes and/or striated surfaces containing east-west trending subhorizontal slickenside striations (Figures 4d and 6d) are associated with fine-grained foliated cataclasites and gouges. Considerable lateral variations in thickness (40–100 cm), texture, and clast composition characterize the fault rocks. Indeed, the lower part of fault zone is dominated by grey to dark grey cataclasites and gouges (Figures 6c and 6f) that mainly rework hornfels schists and quartzites of the Verrucano Formation. At microscopic-scale (Figure 6g) fabrics show sharp transitions from clast and/or matrix-supported breccias to very fine grained cataclasites with thin gouge layers. The quartzites immediately below the fault zone are crosscut by a network of millimeter- to centimeter-thick fractures and cataclastic layers. The upper portion of the fault zone consists of yellowish-reddish breccias and cataclasites with thin gouge layers (Figure 6e). The clast compositions indicate derivation mostly from the overlying Upper Cretaceous flysch, which is marked by intense brecciation and eastward imbrications of sedimentary strata at the contact with fault zone. Moreover, the upper portion of the fault zone was extensively affected by significant late fluid circulation, which led to diffuse carbonate replacement that locally almost completely obliterated fault rock fabrics. Channelized fluid circulation throughout the whole fault zone also occurred as indicated by the presence of a calcite-rich vein system, also described by *Collettini et al.* [2006].

4.3. Terra Nera Section

In the Terra Nera section (Figures 2 and 7), the Zuccale Fault separates the Calamita Schist and Calanchiole Marble in the footwall from the Ortano and Tuscan Units in the hanging wall (Figures 7a and 7b).

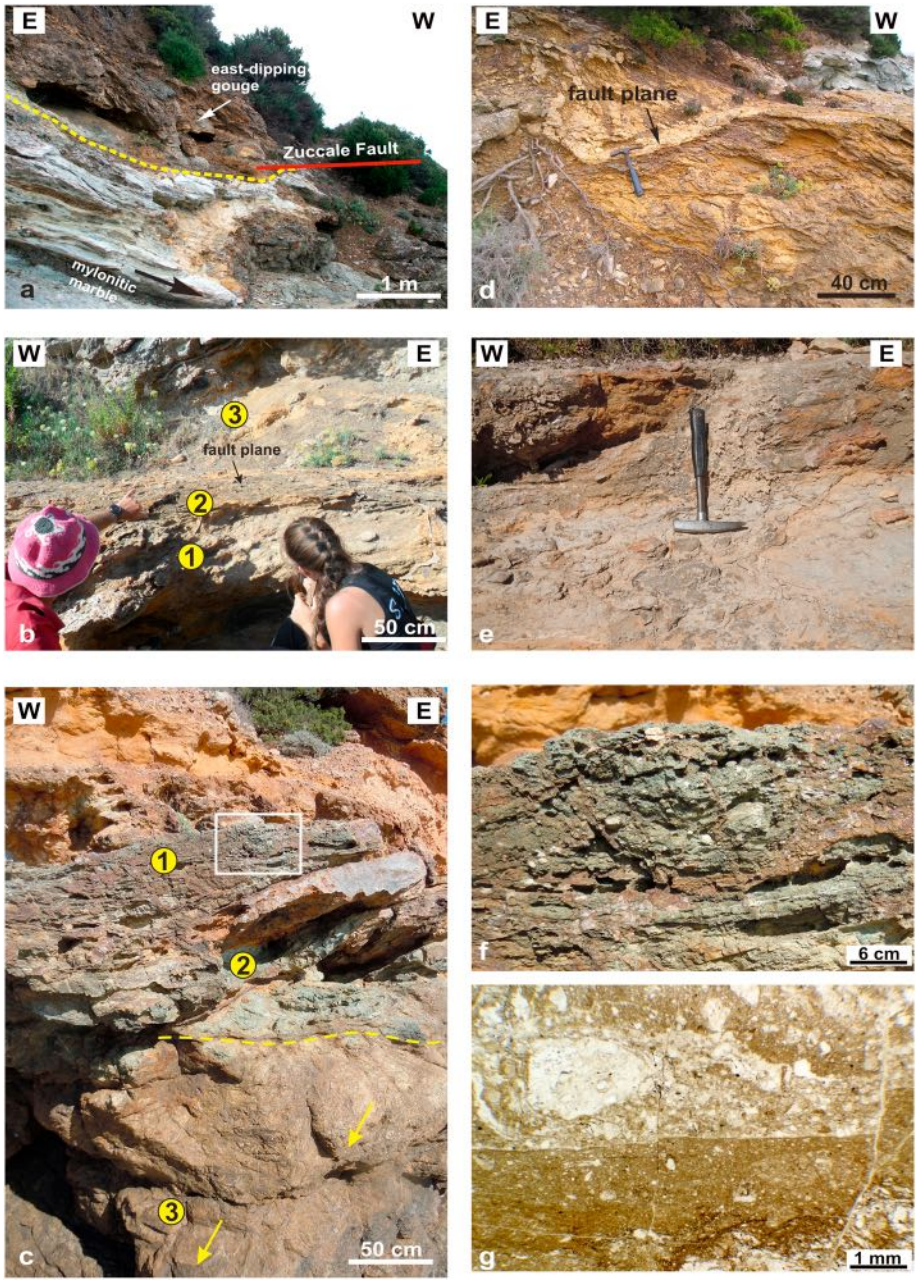

Figure 6. Punta di Zuccale section. (a) Detail of field relationships between west dipping mylonitic marbles (black arrow) of the Calanchiole shear zone (below yellow dashed line) and overlying Zuccale Fault, marked by meter-thick breccias with centimeter-thick east dipping gouge layers. (b) Zuccale Fault cross section with close-up of subhorizontal basal layer of breccias and fine-grained cataclasites (1) reworking footwall rocks (Verrucano Formation quartzites), followed upward by centimeter- to decimeter-thick gouge (2) with striated surfaces. In the background: upper portion of fault zone characterized by yellowish altered cataclasites (3) immediately below the hanging wall (Cretaceous flysch). (c) Detail of basal layer of cataclasites and gouges that discordantly rest on west dipping metamorphic foliation (yellow arrow) of footwall rocks (Verrucano Formation quartzites). (d) Subhorizontal east dipping brittle fault plane crosscutting west dipping metamorphic foliation of strongly altered metasandstone of Verrucano Formation. (e) Detail of fault zone upper portion with brownish breccias containing carbonate clasts of overlying flysch that are crosscut by thin subhorizontal shear planes. (f) Detail of Figure 6c with coarse-grained cataclasites (top middle photo) overlying fine-grained cataclasites and gouges (bottom photo). (g) Microscopic view of fault rock showing sharp transition from fault breccia (top photo) composed of rounded clasts of metamorphic rocks (dominantly quartzites of Verrucano Formation) to cataclasite/gouge (bottom photo) marked by strong comminution of clasts in a fine-grained clay rich matrix.

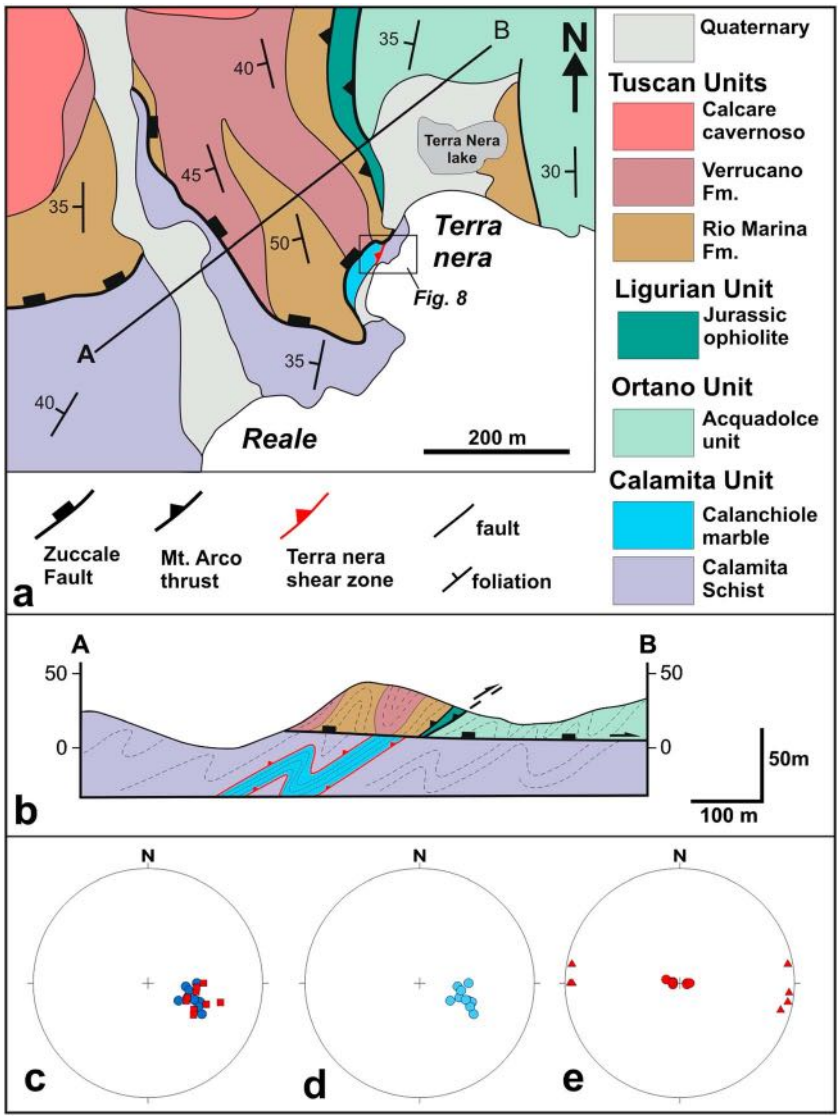

Figure 7. Terra Nera section (see location in Figure 2a). (a) Geological sketch map and (b) cross section of Terra Nera area, (c) equal-area lower hemisphere projections of poles to foliations in the footwall (blue circles) and hanging wall (red circles) of Zuccale Fault, (d) equal-area lower hemisphere projections of poles to foliation in the mylonitic marbles of Terra Nera shear zone, and (e) equal-area lower hemisphere projections of poles to fault planes (red circles) and slickenside striae (red triangles) in the breccias and cataclasites of Zuccale Fault.

The Calamita Schist consists of andalusite-cordierite-bearing hornfels (hornblende hornfels facies) that hosts a diffuse network of late Miocene leucogranitic sills that are associated with the Porto Azzurro pluton (see below). In the footwall of the Zuccale Fault, a NS trending, west dipping ductile shear zone, named here the Terra Nera shear zone, marks the contact between the Calamita Schist and Calanchiole Marble (Figures 7a and 8a). This shear zone consists of diopside-phlogopite-bearing mylonitic marble with boudins of dolomitic marble. The dominant fabric is a west dipping mylonitic foliation (Figures 7b, 7d, and 8b), with synkinematic growth of a calcite + dolomite + phlogopite + diopside ± tremolite mineral assemblage. The marble microstructure is characterized by protomylonitic to mylonitic fabrics marked by coarse-grained (1–2 mm) calcite and dolomite porphyroclasts embedded in a homogeneous matrix of fine-grained (50–80 μm) calcite and dolomite grains. The $^{40}Ar/^{39}Ar$ analysis of synkinematic phlogopite in a sample of mylonitic dolomitic marble (Figure 8b) yielded an age of 6.76 ± 0.08 Ma for the mylonitic fabric in the Terra Nera shear zone (see below). Based on its composition, structural position, and mesoscopic and microscopic fabrics, the mylonitic marble of the Terra Nera shear zone is correlative with the mylonitic

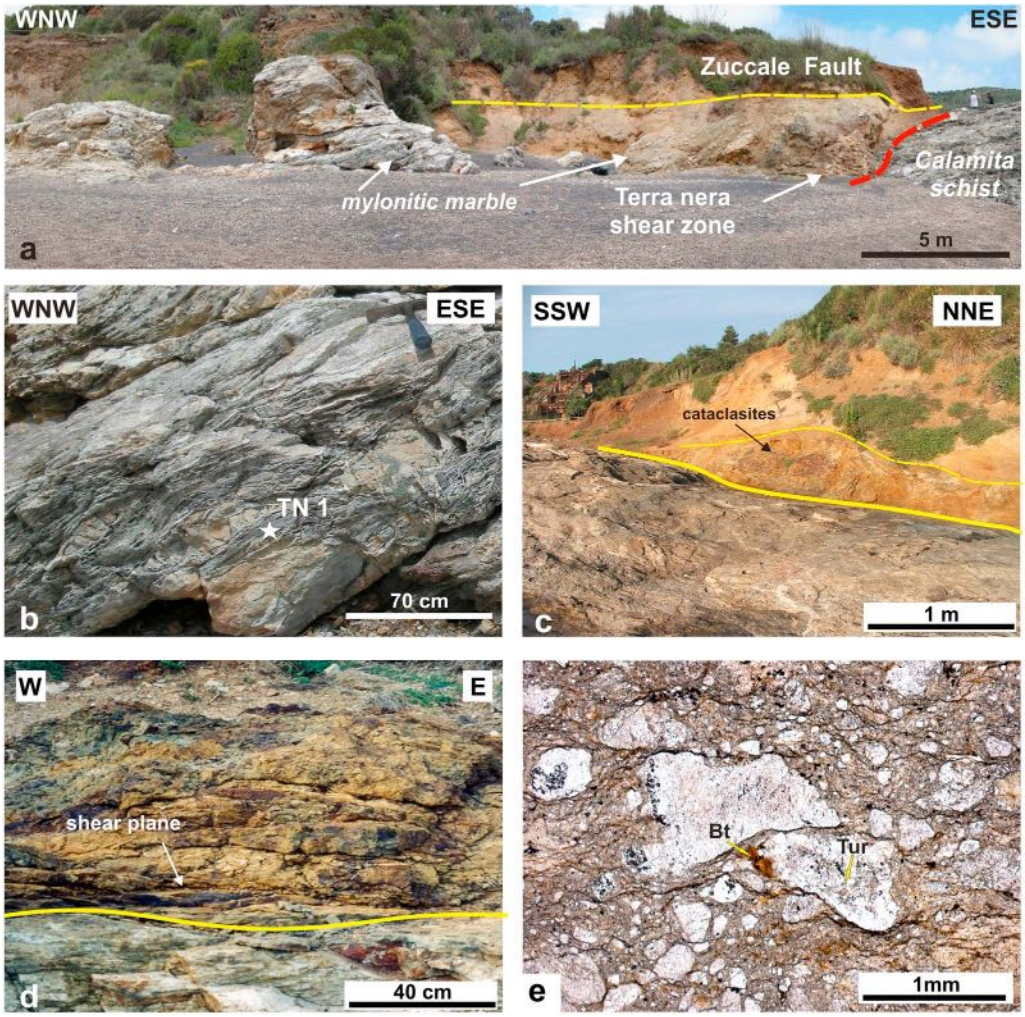

Figure 8. Terra Nera section. (a) Panoramic view of geometric relationships between the Zuccale Fault (yellow line) and the west dipping Terra Nera shear zone (red line) and (b) detail of mylonitic marble at the core of Terra Nera shear zone, showing west dipping foliation and dolomite boudins. The white star is the location of sample TN1 (see supporting information). (c) Outcrop view of the Zuccale Fault (thick yellow line) crosscutting foliation in the Calamita Schist. The fault zone is marked by meter-thick altered cataclasites followed upward by metasandstone of the Verrucano Formation. (d) Detail of well-preserved yellowish gouge layers at the base of the Zuccale Fault, showing centimeter-spaced shear planes gently dipping (5°) toward east. (e) Zuccale Fault breccia composed of rounded clasts of metamorphic (Calamita Schist hornfels) and igneous rocks (leucogranite) in a fine-grained clay rich matrix. Bt: biotite and Tur: tourmaline; scale bar: 1 mm.

marble of the Calanchiole shear zone to the east. As observed at Punta Zuccale, the Terra Nera shear zone is also capped discordantly by the Zuccale Fault (Figures 7a, 7b, and 8a).

In the hanging wall (Figures 7a and 7b) the Acquadolce Unit consists of cordierite-biotite ± andalusite-bearing hornfels and biotite schist (hornblende hornfels facies and albite-epidote hornfels facies), reflecting contact metamorphism related to the emplacement of the Porto Azzurro pluton [*Duranti et al.*, 1992]. The Mount Arco thrust (tectonized serpentinites) occurs structurally above the Acquadolce Unit and forms the base of the Tuscan Units, which consist of thin tectonic slices of Upper Paleozoic-Triassic graphitic phyllites and quartizites of the Rio Marina Formation (Late Carboniferous-Permian) and quartzites of the Verrucano Formation (Middle Triassic), overlain by unmetamorphosed vuggy limestone of the Calcare Cavernoso Formation (Late Triassic). The stratigraphic gap across the Zuccale Fault between the lower and upper complexes is significantly reduced in the Terra Nera section compared to the Buraccio and Punta di Zuccale sections. Indeed, in the Terra Nera section metamorphic rocks of the lower complex (Calamita and Ortano Units; see Figure 2) occur in both the hanging wall (Ortano Unit) and footwall

(Calamita Unit) blocks. Farther along the coast to the northeast of Terra Nera the stratigraphic gap dies out completely, as evidenced by the occurrence of the Calamita Unit with leucogranitic dikes in both the hanging wall and footwall (Figures 2a and 2b).

At map scale, the Zuccale Fault in the Terra Nera section dips gently (~5°) northeast and crosscuts steeper (≥40°) west dipping foliations and tectonic structures in both the footwall and hanging wall blocks (Figures 7a–7c). At the outcrop scale, the fault zone consists of meter-thick, yellowish cataclasites (Figure 8c) with centimeter-thick gouge layers (Figure 8d). In the cataclasites and gouges the main planar fabric is defined by a subhorizontal to gently west dipping (10°) spaced foliation, which in thin section is characterized by preferred growth of phyllosilicates in a very fine grained matrix. This foliation is crosscut by centimeter-spaced fault planes that strike NS and dip gently east. Well-developed east-west trending slickenside lineations on shear planes (Figure 7e) and kinematic indicators including shear bands are consistent with top-to-the-east displacement. At microscopic scale (Figure 8e), the cataclasites consist of coarse-grained (1.5–0.5 mm), rounded to subrounded clasts of high metamorphic grade hornfels derived from the Calamita Schist in a very fine grained (60–40 μm) clay-rich matrix.

4.4. New Radiometric Data on Footwall Rocks of the Zuccale Fault

In order to constrain the age of the deformation structures described above and to estimate the timing of Zuccale Fault activity, two samples (TN1 and CS16) from the Calamita Unit in the footwall block of Zuccale Fault were selected for $^{40}Ar/^{39}Ar$ dating.

TN1 is a phlogopite-bearing mylonitic dolomitic marble collected from the core of the Terra Nera shear zone, a few meters below the contact with the overlying breccias of the Zuccale Fault. The mineral assemblage in this sample is calcite + dolomite + diopside + phlogopite, and it has a foliated fabric consisting of strained elongated dolomite and calcite porphyroclasts (1.5–0.8 mm) embedded within a homogeneous matrix of fine-grained calcite and dolomite grains (80–50 μm). Phlogopite micas occur as strained porphyroclasts (0.7–0.3 mm) and small grains (150–50 μm) in the matrix. Both porphyroclasts and small grains show a well-developed shape-preferred orientation parallel to and defining the foliation. Coarse-grained calcite and diopside grains occur as large porphyroclasts wrapped by the phlogopite-bearing foliation.

CS16 was collected from a decimeter (0.5–0.8 m) thick leucogranite sill emplaced within the Calamita Schist along the western side of the Calamita Peninsula, a few tens of meters below the Zuccale Fault. The sill comprises fine-grained equigranular aplite with a quartz + k-feldspar + tourmaline assemblage that in the margins is replaced by coarse-grained pegmatite with a quartz + k-feldspar + muscovite + andalusite + tourmaline assemblage. The sill's host rock is cordierite-andalusite hornfels.

Metamorphic phlogopite from sample TN1 and magmatic muscovite from sample CS16 were separated using standard separation techniques and irradiated for 30 h in the TRIGA reactor at the University of Pavia along with the Fish Canyon sanidine fluence monitor. Mineral separates were analyzed by the infrared laser step-heating technique following the procedures described in *Di Vincenzo et al.* [2006] and *Di Vincenzo and Skála* [2009]. Data were corrected for postirradiation decay, mass discrimination effects, isotopes derived from interfering neutron reactions, and blanks (see supporting information; errors are given as 2σ).

4.4.1. Sample TN1

Phlogopite from TN1 gave a discordant age spectrum that, excluding the first four steps, is characterized by low gas yield and low radiogenic Ar contents (see supporting information) and has an overall saddle shape. The minimum of the saddle is given by six contiguous steps, concordant within experimental errors, representing ~58% of the total $^{39}Ar_K$ released and yielding an error-weighted mean age of 6.76 ± 0.08 Ma (MSWD = 1.4; Figure 9a). Note that most of the first low- to intermediate-temperature steps (from 0.2 to 1.48 W laser power) are characterized by higher Ca/K ratios than those expected for phlogopite and are therefore contaminated by a low-K and a high-Ca phase, most probably minor calcite.

4.4.2. Sample CS16

Magmatic muscovite from sample CS16 yielded an internally discordant age profile, that after an initial ascending segment for the first 43% of the total $^{39}Ar_K$ released, yields a concordant segment (~57% of the total $^{39}Ar_K$ released) with an error-weighted mean age of 6.33 ± 0.07 Ma (MSWD = 0.57; Figure 9b).

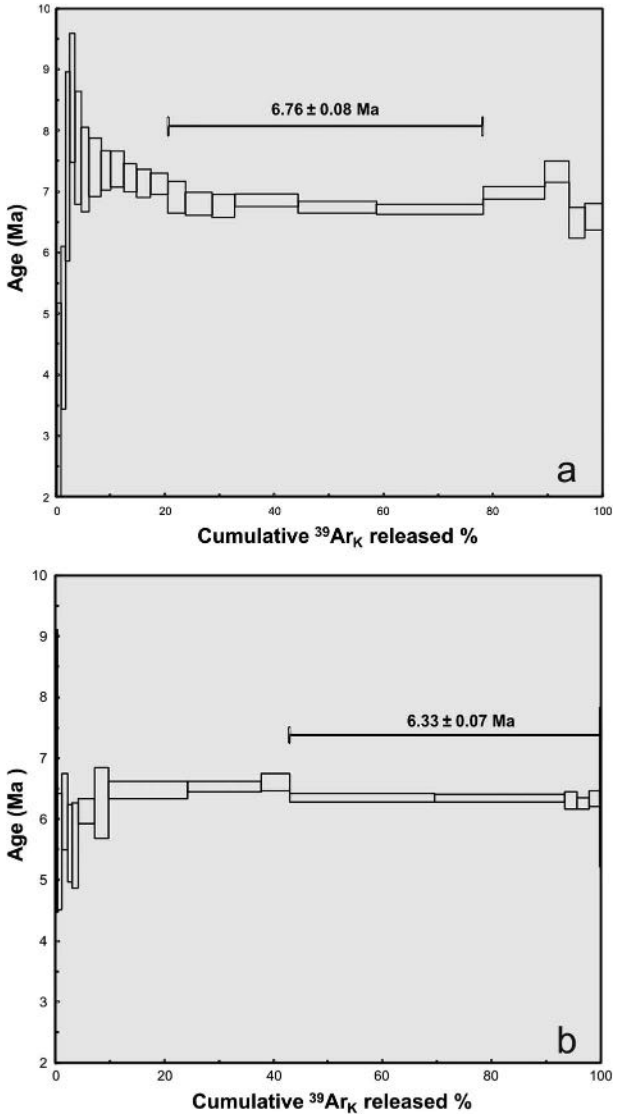

Figure 9. Age release spectrum of (a) TN1 phlogopite and (b) CS16 magmatic muscovite. Box heights indicate the 2σ analytical error.

5. Granite Emplacement in the Calamita Unit

The emplacement of the Porto Azzurro pluton in the Calamita Peninsula of eastern Elba Island (5.9 ± 0.2 Ma ($^{40}Ar/^{39}Ar$ biotite age)) [*Maineri et al.*, 2003] led to the development of a wide contact aureole (~6–7 km in diameter and ~700 m thick) that occurs within the Calamita and Ortano Units (Figure 2a). Contact metamorphic mineral assemblages, dated at 6.2 ± 0.06 Ma ($^{40}Ar/^{39}Ar$ muscovite age [*Musumeci et al.*, 2011]), overprint an early-middle Miocene foliation in the Calamita Schist [*Pertusati et al.*, 1993]. The extent of the contact aureole, which underlies the entire Calamita Peninsula (Figure 2a), indicates that the Porto Azzurro pluton has a much larger subsurface extent than the restricted exposure of medium-grained biotite monzogranite north of the Calamita Peninsula, adjacent to and cut by the trace of the Zuccale Fault (Figures 2 and 3).

Schistose rocks of the Calamita Unit (Figure 2) make up the inner portion of the contact aureole (T_{max} 650°C and $P_{max} < 0.18$–0.2 GPa [*Duranti et al.*, 1992]), where they comprise medium- to high-grade hornfelses [*Mazzarini et al.*, 2011]. The metamorphic grade increases eastward across the Calamita Peninsula, and the highest-grade hornfelses crop out on the eastern coastline where abundant leucogranitic sills and subsidiary dikes derived from the Porto Azzurro pluton intrude them (Figure 2a). Magmatic muscovite from a leucogranite sill emplaced within Calamita Schist yielded an $^{40}Ar/^{39}Ar$ age of 6.33 ± 0.07 Ma (see above).

Foliation attitudes within the Calamita Schist define the large-scale, gently NNW plunging Ripalte antiform cored by high-grade hornfelses (Figure 2a). The Ripalte antiform [*Mazzarini et al.*, 2011] is a steeply inclined, asymmetric fold, overturned toward the east, with gently to moderately dipping foliation in the western backlimb and more steeply dipping foliation in the eastern forelimb (Figure 10b). The latter crops out in the easternmost part of the Calamita Peninsula, extending from Liscoli in the north to Punta delle Ripalte in the south (Figure 2a). The fold axis plunges ~20° north-northwest and the periclinal termination of the fold crops out in the Liscoli area (Figure 2a), where the foliation dips gently to moderately toward the NW and NE. Minor antiforms and synforms as well as reverse faults with top-to-the-east sense of shear occur in the backlimb of the Ripalte antiform. Abundant gently to moderately dipping leucogranitic sills related to the Porto Azzurro pluton are well exposed on the east coast of the Calamita Peninsula, within the eastern forelimb of the Ripalte antiform south of Liscoli, in the western backlimb northwest of Liscoli, and within the northern extent of the periclinal closure between Porto Azzurro and Terra Nera (Figure 2a). The sills vary in length between 175 m and 0.9 m, and their thickness varies from 6.8 m to 0.025 m. Locally, sills are connected by shorter, steeply dipping dikes (Figure 10c), indicating that upward magma transport from the roof of the Porto Azzurro pluton occurred via an interconnected dike-sill network.

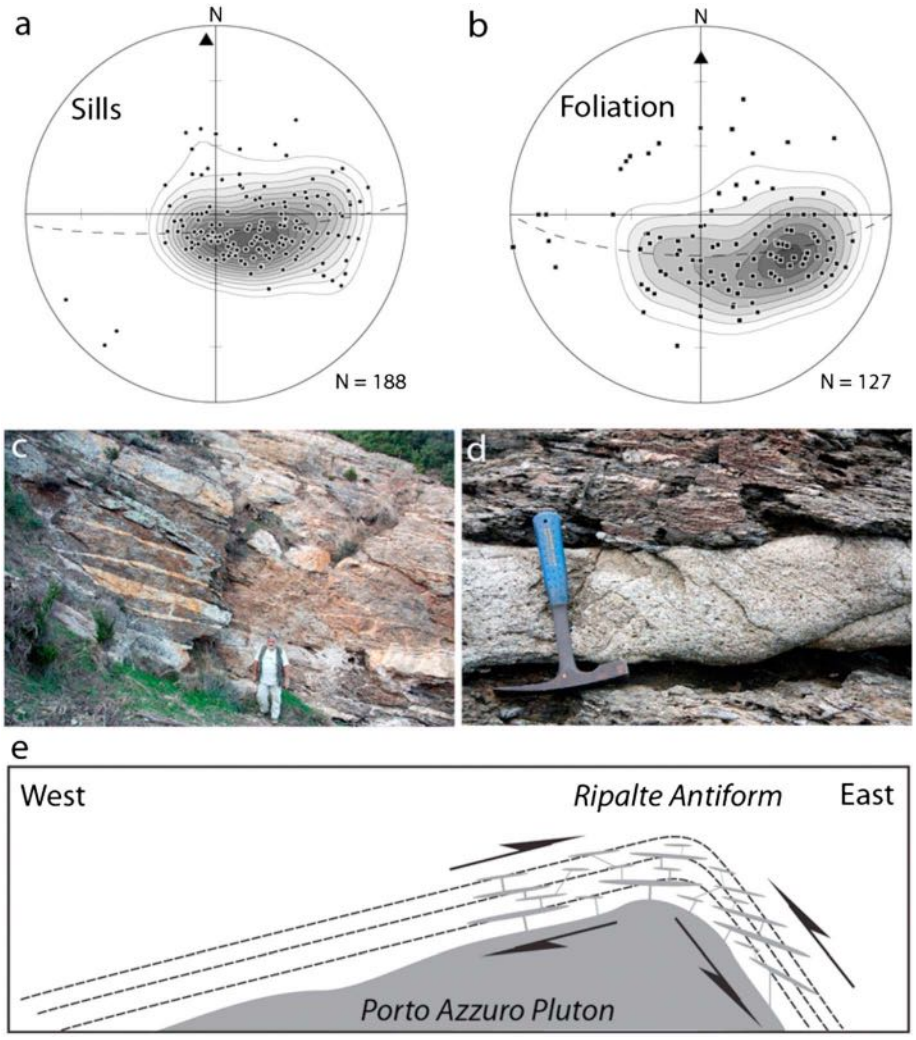

Figure 10. Relationships between leucogranitic sills and wall-rock foliation in the contact aureole of the Porto Azzuro pluton, Calamita Peninsula. (a) Equal-area lower hemisphere stereographic projection of poles to sills. The dashed line is the best fit great circle, and the triangle is its pole. Gaussian contoured with 1 standard deviation contour interval. (b) Equal-area lower hemisphere stereographic projection of poles to foliation in Calamita Schist. The symbols are the same as in Figure 10a. (c) Outcrop photograph showing sill-dike-host-rock foliation relationships. Punta di Buzzancone. Person for scale. (d) Obliquity between sill margins and host-rock foliation. Hammer for scale. (e) Schematic cross section of the Ripalte antiform showing relationships between the folded foliation and sills.

Orientation data suggest that the sills are folded coaxially with the foliation in the Calamita Schist host rocks (Figures 10a and 10b). That is, poles to sills lie on a great circle that shares a common fold axis with the foliation within the host rocks. However, the distribution of poles to sills along the great circle is less than that of the poles to foliation, indicating that their angular dispersion is less than that of the foliation and/or that if the sills are folded, the interlimb angle is greater than that of the folded foliation. Furthermore, in detail the sills are consistently oriented at an oblique angle (8° to 20°) to the host-rock foliation (Figure 10d), and they have statistically shallower dips than the foliation (Figures 10a and 10b). The sense of obliquity between sills and foliation also varies systematically with location within the Ripalte antiform, illustrated schematically in Figure 10e. Southeast of Liscoli in the forelimb the foliation has a mean dip of ~30°ENE and sills have a mean dip of ~14°NE, and the angle between their poles is 15°. In the backlimb northwest of Liscoli the foliation has a mean dip of 33°NW and sills dip ~16°W, with an angular difference of 17°. In the northern part of the periclinal closure between Porto Azzuro and Terra Nera, and away from overprinting steep normal faults, the foliation dips 25° to 45°NE to NNE and sills dip 12° to 40°NE to N, and the mean angle between them is 14°.

6. Discussion

The new geological, structural, and radiometric data presented here have fundamental implications for interpretations of the Zuccale Fault as discussed below.

6.1. Relationships Between Brittle Deformation in the Zuccale Fault and Ductile Deformation in the Footwall

The syncontact metamorphic ductile (mylonitic) fabric in the footwall at Punta di Zuccale is cut and displaced eastward by the Zuccale Fault. Tremolite-talc and/or talc-bearing fine-grained mylonitic marbles are associated with intense strain partitioning within the west dipping Calanchiole shear zone, which significantly predates the Zuccale Fault [*Musumeci and Vaselli*, 2012]. Cataclastic rocks of the Zuccale Fault contain clasts of contact metamorphic rocks (marbles and pelitic hornfels) and granites of the Porto Azzurro pluton. Moreover, in areas where the Zuccale Fault does not crosscut older east vergent thrusts (e.g., Buraccio-Mola section), the internal fault structure comprises breccias and cataclasites without any evidence of ductile deformation (i.e., talc- and/or tremolite-bearing mylonites). Deformation associated with the Zuccale Fault was therefore entirely brittle, and it overprints ductile fabrics that developed during emplacement of the Porto Azzurro Pluton. In addition, although the Zuccale Fault and the older thrusts both display top-to-the-east senses of shear, structural criteria clearly differentiate between the Calanchiole shear zone in the footwall and the Zuccale Fault itself. Indeed, top-to-the-east displacement on the west dipping mylonitic Calanchiole shear zone cuts upward through the lower complex thrust stack, leading to structural thickening of the western side of the contact aureole [*Musumeci and Vaselli*, 2012]. Conversely, top-to-the-east brittle shearing on subhorizontal surfaces within the Zuccale Fault cuts down section in the nappe stack. In the Calanchiole shear zone, top-to-the-east sense of shear can be unequivocally related to horizontal shortening, whereas in the Zuccale Fault the same kinematics are related to either horizontal shortening or extension (see discussion below).

The observations above suggest that mylonitic fabrics in the footwall and the discordant catalastic fault rocks of the Zuccale Fault belong to two different tectonic structures and deformation events that were active at different times under different metamorphic conditions. Our interpretation provides a simple answer to the question posed by *Smith et al.* [2011b], who asked "*why did deformation not simply continue to localize within the talc-phyllonites once they had formed, given that the phyllonites represent an extremely weak horizon capable of accommodating low-angle movements?*" In their reconstruction of the Zuccale Fault, *Smith et al.* [2011b] recognized that deformation was first localized in the tremolite phyllonites and mylonitic marbles and later in the cataclastic rocks. This reconstruction implies a migration of deformation from "weak" phyllonite/mylonite to "hard" cataclasites and breccias. Our new observations indicate that such a migration did not occur during the evolution of a single fault zone because the mylonitic and cataclastic rocks belong to separate deformation events and structures. The previously proposed Zuccale Fault zone architecture with a core of mylonitic rocks and an external portion of cataclastic rocks [*Collettini and Holdsworth*, 2004] is therefore not supported by our recent field observations. In our revised architecture of the Zuccale Fault, talc-rich minerals and fabrics are exclusively associated with an older unrelated structure. Hence, the fault lubrication proposed due to the presence of such mineral phases invoked by *Collettini et al.* [2009] and *Smith et al.* [2011b] is no longer applicable. The proposed architecture of the Zuccale Fault opens questions for the localization and weakening mechanisms in misoriented faults in the upper crust, such as how purely brittle LANFs develop at very shallow crustal levels.

6.2. Relationships Between Granite Emplacement and the Zuccale Fault

It is difficult to reconcile the observed pattern of obliquity between the leucogranitic sills and their host-rock foliation (section 5) with a scenario of (1) prefolding sill emplacement under static conditions or (2) prefolding sill emplacement during unidirectional shearing. In the former scenario, sill injection should have occurred parallel to the strong host-rock anisotropy and no sill-foliation obliquity would be expected. In the latter, sills should form at a constant angle to the host-rock anisotropy during foliation-parallel shear, and this angular relationship should be preserved after folding (i.e., sills will be steeper than the foliation on one limb and shallower on the other). Sill emplacement under conditions of flexural shear during fold amplification and limb steepening provides suitable boundary conditions to form tensile fractures that will have systematically shallower dips than the folded foliation (Figure 10e). Under conditions of magma ingress above a crystallizing pluton during fold amplification, sills will preferentially develop within dilating

Table 1. Radiometric Ages in Samples of Metamorphic and Igneous Rocks in the Footwall and Hanging Wall of the Zuccale Fault[a]

Sample	Locality	Rock Type	Mineral	Method	Age ± σ (Ma)
AZ	Buraccio	monzogranito (PAp) (footwall block)	biotite	^{40}Ar-^{39}Ar	5.9 ± 0.2[b]
CS14	Calamita Peninsula	andalusite-cordierite hornfels (CS) (footwall block)	muscovite	^{40}Ar-^{39}Ar	6.23 ± 0.06[c]
CS12	Calamita Peninsula	andalusite-cordierite hornfels (CS) (footwall block)	zircon	U-Pb	6.40 ± 0.15[c]
TN1	Terra Nera	diopside-flogopite hornfels (CM) (footwall block))	phlogopite	^{40}Ar-^{39}Ar	6.76 ± 0.08[d]
CS16	Calamita Peninsula	leucogranite sill (PAp) (footwall block)	muscovite	^{40}Ar-^{39}Ar	6.33 ± 0.07[d]
RM-L1	Rio Marina	Iron body (VFm) (hanging wall block)	adularia, specularite	U-Th-He	5.39 ± 0.46[e]

[a]PAp: Porto Azzurro pluton, CS: Calamita Schist, CM: Calanchiole Marble, and VFm: Verrucano Formation.
[b]*Maineri et al.* [2003].
[c]*Musumeci et al.* [2011].
[d]This work (see supporting information).
[e]*Lippolt et al.* [1995].

tensile cracks rather than propagating parallel to the host-rock anisotropy. Hence, our preferred interpretation is that the leucogranitic sill network formed synchronously with growth of the Ripalte antiform and crystallization of the Porto Azzurro pluton, well before the development of the Zuccale Fault. Finally, the kilometer-scale amplitude and steeply dipping axial plane of Ripalte antiform, cored by intrusive rocks, and the relationship between the sills and host-rock foliation (Figure 10e), are not compatible with deformation due to vertical shortening caused by pluton inflation, whereas they are consistent with emplacement during folding related to regional crustal shortening [*Cruden et al.*, 2009].

Smith et al. [2011a] have argued that the Porto Azzurro pluton and the associated leucogranitic sill network were emplaced simultaneously with top-to-the-east shearing on the Zuccale Fault. Such a timing relationship is consistent with scenario (2) above, followed by postemplacement folding. However, this sequence of events cannot explain the observed obliquity relationship between sills and foliation in the Calamita Peninsula. Furthermore, as noted above and documented in detail by *Smith et al.* [2011a], the leucogranitic sills are overprinted by brittle faulting, which intensifies northward on the Calamita Peninsula approaching the Zuccale Fault. This is most consistent with activity on the Zuccale Fault and associated footwall brittle deformation postdating the emplacement of both the leucogranitic sills and the Porto Azzurro pluton and EW compression that lead to the growth of the Ripalte antiform.

6.3. Age of Zuccale Fault Activity

Regarding the relative timing of Zuccale Fault activity and emplacement of the Porto Azzuro pluton, the field data presented above demonstrate that (i) Zuccale Fault rocks crosscut felsic intrusive rocks and (ii) fault breccias contain clasts of both felsic intrusive rocks and hornfelses. As shown above, activity on the Zuccale Fault postdates the age of mylonitic fabrics in hornfelses (approximately 6.7 Ma) and the emplacement of felsic leucogranite sills (approximately 6.3 Ma). A further geochronological constraint comes from available (U + Th)-He and K-Ar ages, which yielded an approximately 5.3 Ma age for hydrothermal specularite and adularia in iron-ore deposits within the Rio Marina Formation (eastern Elba), located in the hanging wall of the Zuccale Fault [*Lippolt et al.*, 1995]. The available radiometric data (Table 1) permit two scenarios: (1) the Zuccale Fault displaced both the ore deposits and their host rocks to the east or (2) the ore deposits crosscut the Zuccale Fault. In the former scenario, Zuccale Fault activity must be lower Pliocene (5.3 Ma) or younger in age. In the latter scenario, fault activity is bracketed between the timing of granite emplacement and contact metamorphism (6.7–6.3 Ma) and the formation of iron-ore deposits (5.3 Ma). In either case, the available radiometric ages improve the previous suggestion that the Zuccale Fault was active between 13 Ma and 4 Ma [*Keller and Coward*, 1996; *Collettini*, 2011; *Smith et al.*, 2011a] and suggest a considerably shorter time span for the fault activity.

7. Interpretations of the Zuccale Fault

7.1. Brittle Deformation

The Zuccale Fault is a nearly flat, purely brittle fault zone defined by cataclasites, breccias, and gouges that are up to a few meters thick. The fault zone crosscuts a preexisting stack of tectonic units and intrusive rocks represented by the same westward dipping homoclinal panel of tectonic structures

(imbricate thrusts and foliations) in both the hanging wall and footwall blocks. High-angle fractures and faults in the hanging wall block abut the Zuccale Fault zone, indicating formation by unloading that postdates Zuccale Fault activity.

These characteristics are consistent with an entirely brittle, very shallow crustal level history in which low-temperature frictional processes (cataclastic flow and frictional sliding) were the dominant deformation mechanisms. Moreover, evidence for accommodation of movement within the footwall block is only represented by breccias and cataclasites, without any indication of ductile shear zones. Slip along low-angle faults can be explained by (i) mechanisms that result in postdeformational rotation of the fault plane [e.g., *Wernicke and Axen*, 1988; *Wong and Gans*, 2008] or (ii) by the occurrence of unusual conditions within the fault core, such as locally elevated pore fluid pressures [e.g., *Axen*, 1992], or the presence of low-friction materials [e.g., *Hayman*, 2006; *Collettini et al*., 2009]. According to *Haines et al.* [2014], slip along low-angle faults is possible for dips as low as 16° to 22° for very small coefficients of friction ($\mu = 0.28–0.43$) due the presence of clay-rich gouge.

Postdeformation rotation of the fault plane cannot explain the low dip of the Zuccale Fault because no block tilting has occurred in the hanging wall. Similarly, the purely brittle nature of the Zuccale Fault rocks rules out the possibility of lubrication by low-friction materials (tremolite-talc-bearing mylonites) [e.g., *Collettini et al*., 2009]. The average dip of the Zuccale Fault at macroscopic and mesoscopic scales (5°–10°) also places the fault at the theoretical dip limit of LANFs slipping on clay-rich gouge [*Haines et al*., 2014]. With these points in mind, we hypothesize that a viable mechanism for explaining slip on the Zuccale Fault might be the cyclic presence of high pore fluid pressures in the fault zone, as indicated by vein systems and diffuse fluid alteration.

7.2. Fault Dynamics

The principal geometrical feature of the Zuccale Fault is that it crosscuts the central-eastern Elba Island nappe stack, leading to an apparent attenuation of the original nappe-stack thickness, locally resulting in the juxtaposition of sedimentary units (hanging wall) onto metamorphic units (footwall). However, moving eastward along the slip direction, the attenuation of the nappe-stack thickness dies out progressively such that high metamorphic grade hornfelses of the lower complex (Calamita and Ortano Units) occur in both the hanging wall and footwall along the eastern coast north of Porto Azzurro (see Figures 2 and 7).

This implies that before the development of the Zuccale Fault, (i) metamorphic (lower complex) and sedimentary (upper complex) units were already coupled in a single west dipping tectonic stack, (ii) this stack of tectonic units was at a very shallow crustal level (<0.2 GPa), (iii) the west dipping nappe stack was affected by a large-scale asymmetric antiform coeval with granite emplacement, and (iv) no block rotation was observed in the hanging wall of brittle Zuccale Fault.

The above lines of evidence indicate that the Zuccale Fault accommodates about 6 km of horizontal displacement of a stack of imbricate tectonic units, without the exhumation of footwall rocks.

Considering the west dipping imbrication of tectonic units as the basic geometric constraint for tectonic reconstruction, the flat-lying Zuccale Fault cut downsection through the Elba Island nappe stack in the slip direction. This can be related to either horizontal extension or shortening.

In the case of horizontal extension, the lack of exhumation of deep crustal rocks together with the absence of fault block rotation with axis perpendicular to the slip direction of the fault indicate that the Zuccale Fault should not be considered as a major structure responsible for regional-scale crustal extension [e.g., *Collettini and Holdsworth*, 2004] but rather a minor detachment that accommodates local deformation at uppermost crustal level. According to *Westerman et al.* [2004], in western Elba Island the emplacement of igneous rocks, including the Monte Capanne pluton, as a nested Christmas-tree laccolith complex that led to gravitational collapse accommodated by top-to-the-east low-angle faults, which translated the stack of tectonic units from the west toward eastern Elba Island. In this context, the Zuccale Fault might be considered to be a local extensional fault that developed due to gravitational instability. In this scenario, granite emplacement predates fault activity and is instrumental in promoting the onset of faulting [*Westerman et al*., 2004]. However, the notion of magma emplacement as the driver for the formation of the Zuccale Fault does not account for post-Porto Azzurro pluton emplacement fault activity. Mineral assemblages within the Monte Capanne and Porto Azzurro pluton contact metamorphic aureoles [*Rossetti et al*., 2007; *Duranti et al*., 1992]

indicate that they were emplaced at similar depths. This introduces a substantial challenge for reconstructing a crustal architecture that would result in eastward gravitational collapse.

At larger scale, geophysical data [*Moeller et al*., 2014] indicate that crustal extension in the northern Tyrrhenian Sea significantly decreases from south to north (i.e., from latitude 41°N to the Tuscan shelf). Furthermore, there is no evidence of low-angle fault geometries in seismic reflection profiles, and the total fault displacement is entirely distributed among high-angle faults [*Moeller et al*., 2013]. In the Tuscan shelf at the latitude of Elba Island (approximately 43°N), the reprocessed WSW-ENE CROP M12A seismic reflection line [*Tognarelli et al*., 2011] contains no evidence for east dipping low-angle reflectors. Rather, the acoustic basement (tectonic units of the northern Apennines) and overlying late Neogene sedimentary deposits define a sequence of open antiforms and synforms, which are covered discordantly by subhorizontal reflectors corresponding to Late Pliocene-Quaternary sedimentary deposits. These geophysical observations are not consistent with the occurrence and/or the role of low-angle normal faulting as the main mechanism for crustal extension in the northern Tyrrhenian Sea at the latitude of Elba Island.

Alternatively, the Zuccale Fault could be interpreted as an out-of-sequence thrust. A gently dipping or subhorizontal thrust fault displacing a previous tilted and exhumed stack of tectonic units will result in the apparent attenuation of nappe-stack thickness with local direct superposition of nonmetamorphic over metamorphic rocks [e.g., *Ring et al*., 1999]. This geometry might be easily misattributed to normal faulting, as recently demonstrated by kinematic models of out-of-sequence thrusting [*Pavlis*, 2013]. In this scenario, the exposed flat segment of the Zuccale Fault should connect back to an unexposed west dipping thrust-ramp segment. The possible location of this structure can be inferred by restoring structural markers (i.e., pre-Zuccale Fault thrusts; Figure 2) to their original position and by assuming a horizontal displacement of ~6 km, derived from map-scale separation of markers. Using this approach, the thrust ramp should be located beneath western Elba Island, east of the Mount Capanne pluton. The presence of a thrust ramp in this location could explain the high topographic elevation (above 1000 m) that characterizes western Elba Island. This sector also lies on the Pianosa ridge, a NS striking, positive bathymetric structure extending from Montecristo Island in the south to Capraia Island in the north, which experienced ~3 km of early Pliocene uplift as documented by seismic reflection data [*Mauffret and Contrucci*, 1999].

Our structural data indicate that the Zuccale Fault is a brittle structure that overprints older ductile fabrics (i.e., Calanchiole and Felciaio shear zones). Both the brittle and ductile structures developed over a period of about 1.5–2 Myr that was also syncontact to postcontact metamorphism (Table 1).

The possibility of a continuous top-to-the-east shearing under ductile then brittle deformation conditions should also be considered.

In this case, assuming an extensional setting, footwall exhumation would occur generating significant deformation of the hanging block [e.g., *Axen*, 2004], and sedimentary deposits should record unroofing of the footwall block. In all of the sections of the Zuccale Fault that we have described, both hanging wall and footwall rocks share the same west dipping ductile structures, and no additional deformation within the hanging wall occurred due to extensional displacement on a low-angle fault plane and footwall doming/warping. Moreover, all ductile fabrics (foliations, folds, and thrusts) in the footwall are west dipping along the entire central-eastern Elba Island section of the Zuccale Fault (about 4–5 km; Figures 2a and 2b) and opposite to the slip direction.

Large-scale folds in the footwall block formed by exhumation of ductile crust should be bounded by low-angle ductile to brittle faults that dip toward the direction of shear (e.g., core complexes of North American Cordillera [*Platt et al*., 2014]). Instead, at the Calamita Peninsula, the large-scale asymmetric antiform in the footwall (Ripalte antiform) is beheaded (not bounded) by brittle Zuccale Fault.

Thus, the most likely reconstruction is that the west dipping ductile thrusts and mylonitic foliation (Calanchiole and Felciaio shear zones) and subhorizontal brittle fault (Zuccale Fault) represent ramp and flat segments of a large-scale out-of-sequence thrust zone, which was active during and after the thermal anomaly related to emplacement of the Porto Azzurro pluton and then followed by late purely brittle shear. The kinematic coherence between a west dipping (ductile) ramp and a subhorizontal (brittle) flat therefore favors a shortening environment during continuous ductile to brittle shear.

An interpretation of the Zuccale Fault as an out-of-sequence thrust contradicts the currently accepted model of Neogene crustal extension for the evolution of in the northern Tyrrhenian Sea [e.g., *Carmignani et al*., 1994; *Jolivet et al*., 1998, among many others]. This alternative interpretation is consistent with late Miocene and early Pliocene regional-scale crustal shortening that has been documented in the inner zone of the northern Apennines to affect both the stack of tectonic units and overlying of Neogene sedimentary basins [e.g., *Bonini and Sani*, 2002; *Cerrina Feroni et al*., 2006; *Bonini et al*., 2014]. The emplacement of early Pliocene plutons in this setting occurred in the cores of coeval large-scale antiforms, e.g., Gavorrano antiform and pluton [*Musumeci et al*., 2005, 2008].

Based on the arguments and observations presented above, we propose the following tectonic evolution for the inner portion of northern Apennines:

1. Late Oligocene-early Miocene underplating and accretionary wedge deformation resulted in stacking of Ligurian- and Tuscan-derived units. The deep-seated metamorphic units are characterized by polyphase deformation under HP/LT conditions, with an early generation of structures dated at 27–20 Ma in the metamorphic units of the Apuan Alps [*Carmignani and Kligfield*, 1990].
2. Early-middle Miocene exhumation of metamorphic units occurred during the growth of antiformal stacks and juxtaposed metamorphic and nonmetamorphic units. The exhumation of metamorphic units, dated at 12–11 Ma in the Apuan Alps [*Kligfield et al*., 1986; *Balestrieri et al*., 2003], was driven by extension that has been interpreted as (i) crustal-scale extension in a retro-wedge setting [e.g., *Jolivet et al*., 1998] and/or (ii) local accommodation of gravitational collapse due to overthickening of the accretionary wedge [*Carmignani et al*., 1994]. *Carlini et al*. [2013] and *Clemenzi et al*. [2014] recently documented that overthickening of the orogenic wedge controlled low-angle extensional faults in both Ligurian and Tuscan Units. These new data provide clear evidence for middle Miocene crustal shortening at depth in the inner northern Apennines and coeval gravitational destabilization within the uppermost levels of the orogenic wedge.
3. Late Miocene-early Pliocene crustal shortening resulted in out-of-sequence thrusts that were active during and after magmatic activity in the Tuscan archipelago and southern Tuscany. Likewise, in northern Tuscany (east of the Apuan Alps), middle Miocene low-angle faults (e.g., Val di Lima detachment fault) were successively affected by late Miocene thrusting [*Clemenzi et al*., 2014]. This implies that after wedge reequilibration, crustal shortening was dominant in the northern Apennines. Since the late Pliocene the Apennine chain underwent uplift and extension, accommodated by high-angle normal faulting.

In this evolutionary model the tectonic history of the northern Appenines was dominated by Neogene crustal shortening. Extensional structures can be explained in the context of an accretionary orogenic wedge subjected to large-scale crustal shortening, in which tectonic and gravitational body forces are balanced to maintain the dynamic equilibrium [*Davis et al*., 1983; *Platt*, 1986]. For the hinterland portion of the northern Apennines, the current geodynamic models of (i) middle-late Miocence back-arc extension [e.g., *Jolivet et al*., 1998] and/or (ii) gravitational collapse followed by late Miocene rifting [*Carmignani et al*., 1994] are inconsistent with the geological features documented above in northern and southern Tuscany and the new data reported here for Elba Island. Furthermore, new seismological data image a complex mantle velocity structure beneath the northern Tyrrhenian Sea-northern Appennine system that is not compatible with a simple back-arc setting [*Chiarabba et al*., 2014].

According to *Bonini et al*. [2014], the widespread evidence of shortening phases affecting the hinterland sector of northern Apennines indicates a cessation of extension and a switch to contraction in the late Miocene-early Pliocene. This evolution is currently poorly understood but may be related to a variety of scenarios involving subduction zone blockage [e.g., *Moresi et al*., 2014], with end-members between complete slab detachment and stalled subduction [*Bonini et al*., 2014].

8. Conclusions

Based on new geological and structural data collected from different sections along the fault trace, we have documented a revised architecture for the Zuccale Fault, which comprises only breccias, cataclasites, and gouges. The evidence presented is consistent with the fault forming during a purely brittle deformation event, in which it crosscut previous Miocene tectonic structures and the fault activity postdates the emplacement of the late Miocene Porto Azzurro pluton. We also suggest that movement on the fault may

have been aided in part by intermittent high fluid pressures. The new data have significant implications for fault localization and weakening mechanisms in misoriented faults at upper crustal levels.

We have documented that the occurrence of subhorizontal fault planes in collisional belts with local displacement of nonmetamorphic rocks (hanging wall) onto metamorphic rocks (footwall) are not criteria unique to low-angle normal faults. In order to differentiate between subhorizontal out-of-sequence thrusts and low-angle normal faults, the large-scale structural setting in both the hanging wall and footwall should be considered along with the prefaulting architecture (e.g., of thrusts or nappe stacks). Focusing only on the decimeter- to meter-scale characteristics of the fault zone itself may result in misclassification or conflicting interpretations of fault dynamics and their geological significance.

Although we acknowledge that further investigations are required to better understand the dynamics of the Zuccale Fault, its origin as an out-of-sequence thrust should promote a broader discussion on the late Neogene evolution of the inner zone of the northern Apennines and its geodynamic setting.

Acknowledgments
The authors greatly acknowledge E. Anderson for the fruitful and stimulating discussion about Zuccale Fault architecture and G. Di Vincenzo for providing the Ar/Ar radiometric data. Original data are available upon request to authors. We acknowledge U. Ring, G. Viola, J. Platt, and two anonymous reviewers for their fruitful and constructive revisions: The Associate Editor is also thanked for her effort in manuscript managing.

References

Axen, G. J. (1992), Pore pressure, stress increase and fault weakening in low-angle normal faulting, *J. Geophys. Res.*, *97*(B6), 8979–8991, doi:10.1029/92JB00517.

Axen, G. J. (2004), Mechanics of low-angle normal faults, in *Rheology and Deformation of the Lithosphere at Continental Margins*, Margins: Theoretical and Experimental Earth Science Series, pp. 46–91, Columbia Univ. Press, New York.

Balestrieri, M. L., M. Bernet, M. T. Brandon, V. Picotti, P. W. Reiners, and M. Zattin (2003), Pliocene and Pleistocene exhumation and uplift of two key areas of the northern Apennines, *Quat. Int.*, *101–102*, 67–73.

Barberi, F., G. Giglia, F. Innocenti, G. Marinelli, G. Raggi, C. A. Ricci, P. Squarci, L. Taffi, and L. Trevisan (1967), Carta geologica dell'isola d'Elba scala 1:25.000, C.N.R. Roma.

Barchi, M., C. Pauselli, C. Chiarabba, R. Di Stefano, and C. Federico (2006), Crustal structure, tectonic evolution and seismogenesis in the northern Apennines (Italy), *Boll. Geofis. Teor. Appl.*, *47*(3), 249–270.

Bertini, G., M. Casini, G. Gianelli, and E. Pandeli (2006), Geological structures of a long-living geothermal system, Larderello, Italy, *Terra Nova*, *18*, 163–169.

Boccaletti, M., and F. Sani (1998), Cover thrust reactivations related to internal basement involvement during Neogene-Quaternary evolution of the northern Apennines, *Tectonics*, *17*, 112–130, doi:10.1029/97TC02067.

Boccaletti, M., P. Elter, and G. Guazzone (1971), Plate tectonics model for the development of the western Alps and northern Apennines, *Nature*, *234*, 108–111.

Boccaletti, M., G. Gianelli, and F. Sani (1997), Tectonic regime, granite emplacement and crustal structure in the inner zone of the northern Apennines (Tuscany, Italy): A new hypothesis, *Tectonophysics*, *270*, 127–143.

Boncio, P., F. Brozzetti, and G. Lavecchia (2000), Architecture and seismotectonics of a regional low-angle normal fault zone in central Italy, *Tectonics*, *19*, 1038–1055, doi:10.1029/2000TC900023.

Bonini, M., and F. Sani (2002), Extension and compression in the northern Apennines (Italy) hinterland: Evidence from the late Miocene-Pliocene Siena-Radicofani Basin and relations with basement structures, *Tectonics*, *21*, 1–32, doi:10.1029/2001TC900024.

Bonini, M., F. Sani, E. M. Stucchi, G. Moratti, M. Benvenuti, G. Menanno, and C. Tanini (2014), Late Miocene shortening of the northern Apennines back-arc, *J. Geodyn.*, *74*, 1–31.

Bouillin, J. P. (1983), Exemples de deformation locale liées à la mis en place de granitoides alpins dans des conditions distensives: l'ile d'Elbe (Italie) et le Cap Bougaron (Algérie), *Rev. Geol. Dyn. Geogr. Phys.*, *24*, 101–116.

Carlini, M., A. Artoni, L. Aldega, M. L. Balestrieri, S. Corrado, P. Vescovi, M. Bernini, and L. Torelli (2013), Exhumation and reshaping of far-travelled/allochthonous tectonic units in mountain belts. New insights for the relationships between shortening and coeval extension in the western northern Apennines (Italy), *Tectonophysics*, *608*, 267–287, doi:10.1016/j.tecto.2013.09.029.

Carmignani, L., and R. Kligfield (1990), Crustal extension in the northern Apennines: The transition from compression to extension in the Alpi Apuane core complex, *Tectonics*, *9*, 1275–1303, doi:10.1029/TC009i006p01275.

Carmignani, L., F. A. Decandia, P. L. Fantozzi, A. Lazzarotto, D. Liotta, and M. Meccheri (1994), Tertiary extensional tectonics in Tuscany (northern Apennines, Italy), *Tectonophysics*, *238*, 295–315.

Cerrina Feroni, A., M. Bonini, P. Martinelli, G. Moratti, F. Sani, D. Montanari, and C. Del Ventisette (2006), Lithological control on thrust-related deformation in the Sassa-Guardistallo Basin (northern Apennines hinterland, Italy), *Basin Res.*, *18*, 301–321, doi:10.1111/j.1365-2117.2006.00295.

Chiarabba, C. G., I. B. Giacomuzzi, N. P. Agostinetti, and J. Park (2014), From underplating to delamination-retreat in the northern Apennines, *Earth Planet. Sci. Lett.*, *403*, 108–116, doi:10.1016/j.epsl.2014.06.041.

Clemenzi, L., G. Molli, F. Storti, P. Muchez, R. Swennen, and L. Torelli (2014), Extensional deformation structures within a convergent orogen: The Val di Lima low-angle normal fault system (northern Apennines, Italy), *J. Struct. Geol.*, *66*, 205–222.

Collettini, C. (2011), The mechanical paradox of low-angle normal faults: Current understanding and open questions, *Tectonophysics*, *510*, 253–268, doi:10.1016/j.tecto.2011.07.015.

Collettini, C., and R. E. Holdsworth (2004), Fault zone weakening and character of slip along low-angle normal faults: Insights from the Zuccale Fault, Elba, Italy, *J. Geol. Soc.*, *161*, 1039–1051.

Collettini, C., N. De Paola, and N. R. Goulty (2006), Switches in the minimum compressive stress direction induced by overpressure beneath a low-permeability fault zone, *Terra Nova*, *18*, 224–231, doi:10.1111/j.1365-3121.2006.00683.x.

Collettini, C., C. Viti, S. A. F. Smith, and R. E. Holdsworth (2009), Development of interconnected talc networks and weakening of continental low-angle normal faults, *Geology*, *37*, 567–570.

Cruden, A. R., F. Mazzarini, A. P. Bunger, and G. Musumeci (2009), Geometry, scaling relationships and emplacement dynamics of a ca. 6 Ma shallow felsic sill complex, Calamita Peninsula, Elba Island, Italy, *Eos Trans. AGU, 90*(52), Fall Meet. Suppl., Abstract T13A-p. 1843.

Davis, D., J. Suppe, and F. A. Dahlen (1983), Mechanics of fold-and-thrust belts and accretionary wedges, *J. Geophys. Res.*, *88*, 1153–1172, doi:10.1029/JB088iB02p01153.

Deino, A., J. V. A. Keller, G. Minelli, and G. Pialli (1992), Datazioni $^{40}Ar/^{39}Ar$ del metamorfismo dell'Unità di Ortano-Rio Marina (Isola d'Elba): Risultati preliminari, *Stud. Geol.Camerti*, *2*, 187–192.

Di Vincenzo, G., and R. Skála (2009), $^{40}Ar–^{39}Ar$ laser dating of tektites from the Cheb Basin (Czech Republic): Evidence for coevality with moldavites and influence of the dating standard on the age of the Ries impact, *Geochim. Cosmochim. Acta*, *73*, 493–513.

Di Vincenzo, G., S. Tonarini, B. Lombardo, D. Castelli, and L. Ottolini (2006), Comparison of ^{40}Ar-^{39}Ar and Rb-Sr data on phengites from the UHP Brossasco-Isasca Unit (Dora Maira Massif, Italy): Implications for dating white mica, *J. Petrol.*, *47*, 1439–1465.

Dini, A., F. Innocenti, S. Rocchi, S. Tonarini, and D. S. Westerman (2002), The magmatic evolution of the late Miocene laccolith–pluton–dyke granitic complex of Elba Island, Italy, *Geol. Mag.*, *139*, 257–279.

Duranti, S., R. Palmeri, P. C. Pertusati, and C. A. Ricci (1992), Geological evolution and metamorphic petrology of the basal sequence of eastern Elba (complex II), *Acta Vulcanologica*, *2*, 213–229.

Elter, P. (1975), Introduction a` la géologie de l'Apennin septentrional, *Bull. Soc. Geol. Fr.*, *7*, 956–962.

Garfagnoli, F., E. Menna, E. Pandeli, and G. Principi (2005), The Porto Azzurro Unit (Mt. Calamita promomtory, south-eastern Elba Island, Tuscany): Stratigraphic, tectonic and metamorphic evolution, *Boll. Soc. Geol. Ital.*, *3*, 119–138.

Giorgetti, G., B. Goffe, I. Memmi, and F. Nieto (1998), Metamorphic evolution of Verrucano metasediments in northern Apennines: New petrological constraints, *Eur. J. Mineral.*, *10*, 1295–1308.

Haines, S. H., B. Kaproth, C. Marone, D. Saffer, and B. van der Pluijm (2014), Shear zones in clay-rich fault gouge: A laboratory study of fabric development and evolution, *J. Struct. Geol.*, *51*, 206–225, doi:10.1016/j.jsg.2013.01.002.

Hayman, N. (2006), Shallow crustal faults from the Black Mountain detachments, Death Valley, Calif., *J. Struct. Geol.*, *28*, 1767–1784.

Jolivet, L., et al. (1998), Midcrustal shear zones in postorogenic extension: Example from the Tyrrhenian Sea, *J. Geophys. Res.*, *103*, 12,123–12,160, doi:10.1029/97JB03616.

Keller, J. V. A., and M. P. Coward (1996), The structure and evolution of the northern Tyrrhenian Sea, *Geol. Mag.*, *103*, 1–16.

Keller, J. V. A., and G. Pialli (1990), Tectonics of the island of Elba: A reappraisal, *Boll. Soc. Geol. Ital.*, *109*, 413–425.

Kligfield, R., J. Hunziker, R. D. Dallmeyer, and S. Schamel (1986), Dating of deformation phases using K-Ar and $^{40}Ar/^{39}Ar$ techniques: Results from the northern Apennines, *J. Struct. Geol.*, *8*, 781–798.

Lippolt, H. J., R. S. Wernicke, and R. Bahr (1995), Paragenetic specularite and adularia (Elba, Italy): Concordant (U + Th)–He and K-Ar ages, *Earth Planet. Sci. Lett.*, *132*, 43–51.

Maineri, C., M. Benvenuti, P. Costagliola, A. Dini, P. Lattanzi, C. Ruggieri, and I. M. Villa (2003), Sericitic alteration at the La Crocetta mine (Elba Island, Italy): Interplay between magmatism, tectonics, and hydrothermal activity, *Miner. Deposita*, *38*, 67–86.

Malinverno, A., and W. B. F. Ryan (1986), Extension on the Tyrrhenian Sea and shortening in the Apennines as result of arc migration driven by sinking of the lithosphere, *Tectonics*, *5*, 227–245, doi:10.1029/TC005i002p00227.

Mauffret, A., and I. Contrucci (1999), Crustal structure of the North Tyrrhenian Sea: First result of the multichannel seismic LISA cruise, in *The Mediterranean Basins: Tertiary Extension Within the Alpine Orogen*, edited by B. Durand et al., *Geol. Soc. London Spec. Publ.*, *156*, 169–193.

Mazzarini, F., G. Musumeci, and A. R. Cruden (2011), Vein development during folding in the upper brittle crust: The case of tourmaline-rich veins of eastern Elba Island, northern Tyrrhenian Sea, Italy, *J. Struct. Geol.*, *33*, 1509–1522, doi:10.1016/j.jsg.2011.07.001.

Mirabella, F., F. Brozzetti, A. Lupattelli, and M. R. Barchi (2011), Tectonic evolution of a low-angle extensional fault system from restored cross-sections in the northern Apennines (Italy), *Tectonics*, *30*, TC6002, doi:10.1029/2011TC002890.

Moeller, S., I. Grevemeyer, C. R. Ranero, C. Berndt, D. Klaeschen, V. Sallares, N. Zitellini, and R. de Franco (2013), Early-stage rifting of the northern Tyrrhenian Sea Basin: Results from a combined wide-angle and multichannel seismic study, *Geochem. Geophys. Geosyst.*, *14*, 3032–3052, doi:10.1002/ggge.20180.

Moeller, S., I. Grevemeyer, C. R. Ranero, C. Berndt, D. Klaeschen, V. Sallares, N. Zitellini, and R. de Franco (2014), Crustal thinning in the northern Tyrrhenian Rift: Insights from multichannel and wide-angle seismic data across the basin, *J. Geophys. Res. Solid Earth*, *119*, 1655–1677, doi:10.1002/2013JB010431.

Molli, G., G. Giorgetti, and M. Meccheri (2002), Tectonometamorphic evolution of the Alpi Apuane Metamorphic Complex: New data and constraints for geodynamic models, *Boll. Soc. Geol. Ital.*, *1*, 789–800.

Moresi, L., P. G. Betts, M. S. Miller, and R. Cayley (2014), Dynamics of continental accretion, *Nature*, *508*, 245–248, doi:10.1038/nature13033.

Musumeci, G., and L. Vaselli (2012), Neogene deformation and granite emplacement in the metamorphic units of northern Apennines (Italy): Insights from mylonitic marbles in the Porto Azzurro pluton contact aureole (Elba Island), *Geosphere*, *8*(2), 470–490, doi:10.1130/GES00665.1.

Musumeci, G., F. Mazzarini, G. Corti, M. Barsella, and D. Montanari (2005), Magma emplacement in a thrust ramp anticline: The Gavorrano Granite (northern Apennines, Italy), *Tectonics*, *24*, TC6009, doi:10.1029/2005TC001801.

Musumeci, G., F. Mazzarini, and M. Barsella (2008), Pliocene crustal shortening on the Tyrrhenian side of the northern Apennines: Evidence from the Gavorrano antiform (southern Tuscany, Italy), *J. Geol. Soc. London*, *165*, 105–114.

Musumeci, G., F. Mazzarini, M. Tiepolo, and G. Di Vincenzo (2011), U-Pb and ^{40}Ar-^{39}Ar geochronology of Palaeozoic units in the northern Apennines: Determining protolith age and Alpine evolution using the Calamita Schist and Ortano Porphyroid, *Geol. J.*, *46*, 288–310, doi:10.1002/gj.1266.

Pavlis, T. (2013), Kinematic model for out-of-sequence thrusting: Motion of two ramp-flat faults and the production of upper plate duplex systems, *J. Struct. Geol.*, *51*, 132–143.

Pertusati, P. C., G. Raggi, C. A. Ricci, S. Duranti, and R. Palmeri (1993), Evoluzione postcollisionale dell'Elba centro-orientale, *Mem. Soc. Geol. Ital.*, *49*, 297–312.

Platt, J. P. (1986), Dynamics of orogenic wedges and the uplift of high-pressure metamorphic rocks, *Geol. Soc. Am. Bull.*, *97*, 1037–1053.

Platt, J. P., W. M. Behr, and F. J. Cooper (2014), Metamorphic core complexes: Windows into the mechanics and rheology of the crust, *J. Geol. Soc.*, *172*, 9–27, doi:10.1144/jgs2014-036.

Ring, U., M. T. Brandon, S. D. Willet, and G. S. Lister (1999), Exhumation processes, in *Exhumation Processes, Normal Faulting, Ductile Flow and Erosion*, edited by U. Ring et al., *Geol. Soc. London Spec. Publ.*, *154*, 1–27.

Rosenbaum, G., and G. S. Lister (2004), Neogene and Quaternary rollback evolution of the Tyrrhenian Sea, the Apennines and the Sicilian Maghrebides, *Tectonics*, *23*, TC1013, doi:10.1029/2003TC001518.

Rosenbaum, G., M. Gasparon, F. P. Lucente, A. Peccerillo, and M. S. Miller (2008), Kinematics of slab tear during subduction and implications for Italian magmatism, *Tectonics*, *27*, TC2008, doi:10.1029/2007TC002143.

Rossetti, F., F. Tecce, A. Billi, and M. Brilli (2007), Patterns of fluid flow in the contact aureole of the late Miocene Monte Capanne pluton (Elba Island, Italy): The role of structures and rheology, *Contrib. Mineral. Petrol.*, *153*, 743–760, doi:10.1007/s00410-006-0175-3.

Serri, G., F. Innocenti, and P. Manetti (1993), Geochemical and petrological evidence of the subduction of delaminated Adriatic continental lithosphere in the genesis of the Neogene–Quaternary magmatism of central Italy, *Tectonophysics*, *223*, 117–147.

Smith, S. A. F., and D. Faulkner (2010), Laboratory measurements of the frictional properties of the Zuccale low-angle normal fault, Elba Island, Italy, *J. Geophys. Res.*, *115*, B02407, doi:10.1029/2008JB006274.

Smith, S. A. F., R. E. Holdsworth, and C. Collettini (2011a), Interactions between low-angle normal faults and plutonism in the upper crust: Insights from the Island of Elba, Italy, *Geol. Soc. Am. Bull.*, *123*(1/2), 329–346, doi:10.1130/B30200.1.

Smith, S. A. F., R. E. Holdsworth, C. Collettini, and M. A. Pearce (2011b), The microstructural character and mechanical significance of fault rocks associated with a continental low-angle normal fault: The Zuccale Fault, Elba Island, Italy, in *Geology of the Earthquake Source: A Volume in Honour of Rick Sibson*, edited by A. Fagereng et al., *Geol. Soc. London Spec. Publ.*, *359*, 97–113, doi:10.1144/SP359.6.

Theye, T., J. Reinhardt, B. Goffe, L. Jolivet, and C. Brunet (1997), Ferro and magnesio carpholite from the Monte Argentario (Italy): First evidence for high-pressure metamorphism of the metasedimentary Verrucano sequence, and significance for *P-T* path reconstruction, *Eur. J. Mineral.*, *9*, 859–873.

Tognarelli, A., E. Stucchi, G. Musumeci, F. Mazzarini, and F. Sani (2011), Reprocessing of the CROP M12A seismic line focused on shallow-depth geological structures in the northern Tyrrhenian Sea, *Boll. Geofis.Teor. Appl.*, *52*, 23–38.

Wernicke, B., and G. J. Axen (1988), On the role of isostasy in the evolution of normal fault systems, *Geology*, *16*(9), 848–851, doi:10.1130/0091-7613.

Westerman, D. S., A. Dini, F. Innocenti, and S. Rocchi (2004), Rise and fall of a nested Christmas-tree laccolith complex, Elba Island, Italy, in *Physical Geology of High-Level Magmatic Systems*, edited by C. Breitkreuz and N. Petford, *Geol. Soc. London Spec. Publ.*, *234*, 195–213.

Wise, D. U., D. E. Dunn, J. T. Engelder, P. A. Geiser, R. D. Hatcher, S. A. Kish, A. L. Odom, and S. Schamel (1974), Fault-related rocks: Suggestions for terminology, *Geology*, *12*, 391–394.

Wong, M. S., and P. B. Gans (2008), Geologic, structural, and thermochronologic constraints on the tectonic evolution of the Sierra Mazata´n core complex, Sonora, Mexico: New insights into metamorphic core complex formation, *Tectonics*, *27*, TC4013, doi:10.1029/2007TC002173.